

AD-A157 684

STUDIES ON AMORPHIZING SILICON USING SILICON ION
IMPLANTATION(U) AIR FORCE WRIGHT AERONAUTICAL LABS
WRIGHT-PATTERSON AFB OH N C FERNELIUS ET AL APR 85

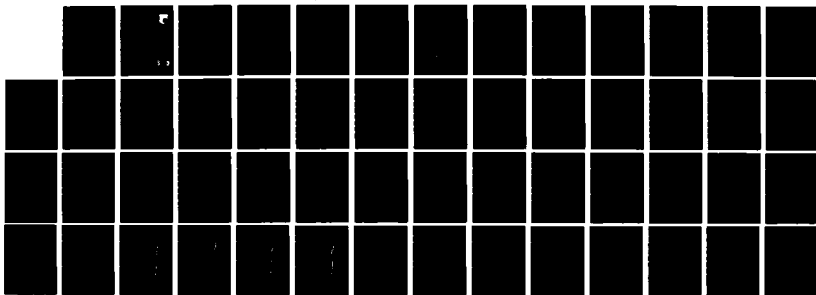
1/1

UNCLASSIFIED

AFMRL-TR-84-4115

F/G 20/12

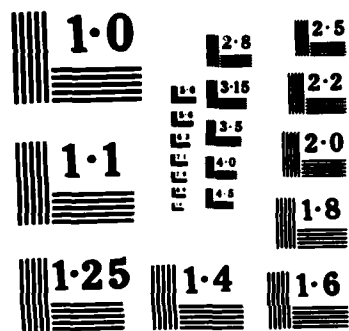
NL



END

FILMED

DTIC



NATIONAL BUREAU OF STANDARDS
MICROCOPY RESOLUTION TEST CHART

AD-A157 684

STUDIES ON AMORPHIZING SILICON USING SILICON ION IMPLANTATION

Nils C. Fernelius
Timothy L. Peterson
Melvin C. Ohmer, et al.

Laser and Optical Materials Branch
Electromagnetic Materials Division

April 1985

Interim Report for Period July 1983 - July 1984



Approved for public release; distribution unlimited.

DTIC FILE COPY

MATERIALS LABORATORY
AIR FORCE WRIGHT AERONAUTICAL LABORATORIES
AIR FORCE SYSTEMS COMMAND
WRIGHT-PATTERSON AIR FORCE BASE, OHIO 45433

DTIC
ELECTE
JUL 17 1985
S G D

85 06 28 051

NOTICE


When Government drawings, specifications, or other data are used for any purpose other than in connection with a definitely related Government procurement operation, the United States Government thereby incurs no responsibility nor any obligation whatsoever; and the fact that the government may have formulated, furnished, or in any way supplied the said drawings, specifications, or other data, is not to be regarded by implication or otherwise as in any manner licensing the holder or any other person or corporation, or conveying any rights or permission to manufacture use, or sell any patented invention that may in any way be related thereto.

This report has been reviewed by the Office of Public Affairs (ASD/PA) and is releasable to the National Technical Information Service (NTIS). At NTIS, it will be available to the general public, including foreign nations.

This technical report has been reviewed and is approved for publication.



TIMOTHY L. PETERSON
Project Monitor
Laser & Optical Materials Branch



G. EDWARD KUHL, Chief
Laser & Optical Materials Branch
Electromagnetic Materials Division

FOR THE COMMANDER



MERRILL L. MINGES, Chief
Electromagnetic Materials Division
Materials Laboratory
AF Wright Aeronautical Laboratories

"If your address has changed, if you wish to be removed from our mailing list, or if the addressee is no longer employed by your organization please notify AFWAL/MLPO, W-PAFB, OH 45433 to help us maintain a current mailing list".

Copies of this report should not be returned unless return is required by security considerations, contractual obligations, or notice on a specific document.

UNCLASSIFIED

SECURITY CLASSIFICATION OF THIS PAGE

REPORT DOCUMENTATION PAGE

1a. REPORT SECURITY CLASSIFICATION UNCLASSIFIED			1b. RESTRICTIVE MARKINGS	
2a. SECURITY CLASSIFICATION AUTHORITY			3. DISTRIBUTION/AVAILABILITY OF REPORT	
2b. DECLASSIFICATION/DOWNGRADING SCHEDULE			Approved for public release; distribution unlimited.	
4. PERFORMING ORGANIZATION REPORT NUMBER(S) AFWAL-TR-84-4115			5. MONITORING ORGANIZATION REPORT NUMBER(S)	
6a. NAME OF PERFORMING ORGANIZATION Materials and Avionics Labs Air Force Wright Aeronautical Laboratories, AFSC		6b. OFFICE SYMBOL (If applicable) AFWAL/MLPO		7a. NAME OF MONITORING ORGANIZATION
6c. ADDRESS (City, State and ZIP Code) AFWAL/MLPO Wright-Patterson AFB, OH 45433			7b. ADDRESS (City, State and ZIP Code)	
8a. NAME OF FUNDING/SPONSORING ORGANIZATION		8b. OFFICE SYMBOL (If applicable)		9. PROCUREMENT INSTRUMENT IDENTIFICATION NUMBER
8c. ADDRESS (City, State and ZIP Code)			10. SOURCE OF FUNDING NOS.	
			PROGRAM ELEMENT NO.	PROJECT NO.
			61102F	2306
			TASK NO.	2306Q
			WORK UNIT NO.	2306Q106
11. TITLE (Include Security Classification) STUDIES ON AMOR- PHIZING SILICON USING SILICON ION IMPLANTATION				
12. PERSONAL AUTHOR(S) Nils C. Fernelius, Timothy L. Peterson, Melvin C. Ohmer, David C. Ingram, Anthony W. McCormick, and James E. Ehret				
13a. TYPE OF REPORT Interim		13b. TIME COVERED FROM Jul 83 TO Jul 84		14. DATE OF REPORT (Yr., Mo., Day) April 1985
				15. PAGE COUNT 56
16. SUPPLEMENTARY NOTATION				
17. COSATI CODES			18. SUBJECT TERMS (Continue on reverse if necessary and identify by block number)	
FIELD	GROUP	SUB. GR.		
20	12		Ion Implantation, Silicon, Amorphous, Rutherford	
20	02		Backscattering, Thin Films	
19. ABSTRACT (Continue on reverse if necessary and identify by block number)				
<p>Studies of various conditions to create amorphous Si regions suitable for recrystallization of 0.3 micron and 0.5 micron Si films were made on the Varian 400-10AR Ion Implanter in the Avionics Laboratory and on the General Ionex Corporation 1.7 MeV Tandetron accelerator at Universal Energy Systems. Experimentally, cooling the sample substrate was found to be very important to achieving amorphous regions in the sample. Toward the end of this effort, Dow Corning heat sink compound RTV 340 was found to be a superior mounting medium to rubber cement.</p> <p style="text-align: right;">(Continued on Back)</p>				
20. DISTRIBUTION/AVAILABILITY OF ABSTRACT			21. ABSTRACT SECURITY CLASSIFICATION	
UNCLASSIFIED/UNLIMITED <input checked="" type="checkbox"/> SAME AS RPT. <input type="checkbox"/> DTIC USERS <input type="checkbox"/>			UNCLASSIFIED	
22a. NAME OF RESPONSIBLE INDIVIDUAL Nils Fernelius			22b. TELEPHONE NUMBER (Include Area Code) (513) 255-4474	22c. OFFICE SYMBOL AFWAL/MLPO

DD FORM 1473, 83 APR

EDITION OF 1 JAN 73 IS OBSOLETE.

SECURITY CLASSIFICATION OF THIS PAGE

On the Varian Implanter for samples mounted with rubber cement and with liquid nitrogen in the dewar. The following combinations of ion energy and dosage amorphized the desired regions. For 0.3 micron thick Silicon films:

5×10^{14} ions/cm ²	@ 150 keV
5×10^{14}	@ 180
2×10^{14}	@ 200

For 0.5 micron thick Silicon films:

5×10^{14} ions/cm ²	@ 250 keV
5×10^{14}	@ 275
$2 \times 10^{14} / 2 \times 10^{14}$	@ 300 keV/120 keV

To achieve an amorphous region at a given depth in a Si sample by implanting Si ions, the necessary parameters to specify are the implant ion energy, dosage and substrate temperature.

Except for the lowest energy case, no amorphous regions were obtained on samples implanted by the Tandetron, which had no provision at that time for cooling samples.

FOREWORD

This report describes an in-house effort conducted by personnel of the Laser and Optical Materials Branch (MLPO), Electromagnetic Materials Division (MLP), Materials Laboratory, in collaboration with personnel of the Electronic Research Branch (AADR), Avionics Laboratory. All are parts of the Air Force Wright Aeronautical Laboratories (AFWAL), Wright-Patterson Air Force Base, Ohio 45433. Part of the work was performed by Universal Energy Systems, 4401 Dayton-Xenia Road, Dayton, Ohio 45432. David C. Ingram was supported by the Visiting Scientist program of the Materials Laboratory, Contract F 33615-82-C-5001. Nils C. Fernelius is a National Research Council Senior Research Associate.

The work reported herein was performed during the period July 1983 to July 1984 by the authors. It is part of the Laser Annealing Project of Work Unit Directive 48 - Electro-Optical Materials, Job Order Number 2306Q106.

TABLE OF CONTENTS

SECTION	PAGE
I INTRODUCTION	1
1. Silicon Films	1
2. Ion Implantation	2
3. Damage Distribution and Atomic Displacement Due to Ion Implantation	7
4. Rutherford Backscattering and Channeling	8
II EXPERIMENTAL WORK	12
III SUMMARY AND CONCLUSIONS	40
IV RECOMMENDATIONS	41
REFERENCES	42

Accession For	
NTIS GRA&I	<input checked="" type="checkbox"/>
DTIC TAB	<input type="checkbox"/>
Unannounced	<input type="checkbox"/>
Justification	
By _____	
Distribution/	
Availability Codes	
Dist	Avail and/or Special
A/	



LIST OF ILLUSTRATIONS

FIGURE		PAGE
1	Plots of Nuclear Energy Loss S_n , Electronic Energy Loss S_e , and Projected Range R_e for Si Into Si Taken from B. Smith Ion Implantation Range Data for Silicon and Germanium Device Technology (1977)	6
2	Schematic Rutherford Backscattering Yield Plots for Random and Aligned Directions Versus Energy	9
3	Definition of Angles and Depths in Rutherford Backscattering Measurements	11
4	Si Into Si Implants Using Varian Machine. 150 keV Incident Ion Energy at $1, 2 \text{ \& } 5 \times 10^{14}$ Ions/cm ² Doses. LN ₂ in Dewar	13
5	Si Into Si Implants Using Varian Machine. 200 keV Incident Ion Energy at $0.5, 1, 2, \text{ \& } 5 \times 10^{14}$ Ions/cm ² . LN ₂ in Dewar	14
6	Si Into Si Implants Using Varian Machine. 250 keV Incident Ion Energy at $1 \text{ \& } 2 \times 10^{14}$ Ions/cm ² . LN ₂ in Dewar	15
7	Si Into Si Implants Using Varian Machine. 180 keV @ 5×10^{14} Ions/cm ² . LN ₂ in Dewar	17
8	Si Into Si Using Varian Machine. 180 keV @ 1×10^{15} Ions/cm ² . LN ₂	18
9	Si Into Si On Varian Machine. 250 keV @ 5×10^{14} Ions/cm ² LN ₂ in Dewar	19
10	Si Into Si On Varian Machine. 275 keV @ 5×10^{14} Ions/cm ² . LN ₂	20
11	Si Into Si On Varian Machine. 275 keV @ 1×10^{15} Ions/cm ² . LN ₂	21
12	Si Into Si On Varian Machine. 300 keV @ 2×10^{14} Ions/cm ² . LN ₂	22
13	Si Into Si On Varian Machine. 300 keV/120 keV @ $2 \times 10^{14} / 2 \times 10^{14}$ Ions/cm ² . LN ₂ in Dewar	23
14	Si Into Si On Varian Machine. 300 keV @ 5×10^{14} Ions/cm ² . LN ₂	24
15	Si Into Si On Varian Machine. 325 keV @ 1×10^{15} Ions/cm ² . LN ₂	25

LIST OF ILLUSTRATIONS (Cont'd)

FIGURE		PAGE
16	Si Into Si Using Tandetron. 180 keV Incident Ion Beam Energy With 1×10^{15} Ions/cm ² Dose. Initially at Room Temperature	26
17	Si Into Using Tandetron. 250 keV @ 5×10^{14} . Room Temperature	27
18	Si Into Using Tandetron. 300 keV @ 2×10^{14} Ions/cm ² . Room Temperature	28
19	Si Into Si Using Tandetron. 300 keV @ 5×10^{14} Ions/cm ² Room Temperature	29
20	Si Into Si Using Varian Machine. 180 keV Incident Ion Beam Energy With 1×10^{15} Ions/cm ² . Dow Corning 340 Mounting. Room Temperature	31
21	Si Into Si Implants Using Varian Machine. 180 keV Incident Ion Beam Energy With 1×10^{15} Ions/cm ² Dose. Rubber Cement Mounting. Initially at Room Temperature	32
22	Si Into Si On Varian Machine. 300 keV @ 5×10^{14} Ions/cm ² . Dow Corning 340 Mounting. Room Temperature	33
23	Si Into Si On Varian Machine. 300 keV @ 5×10^{14} Ions/cm ² . Rubber Cement Mounting. Room Temperature	34
24	Si Into Si On Varian Machine. 250 keV @ 5×10^{14} Ions/cm ² . Rubber Cement Mounting. Room Temperature	35
25	Si Into Si On Varian Machine. 300 keV @ 2×10^{14} Ions/cm ² . Rubber Cement Mountin g. Room Temperature	36

LIST OF TABLES

TABLE		PAGE
1	Summary of SOS Recrystallization Techniques Using Si^+ Implantation and Heat Treatments	3
2	Summary of Si Implant Conditions in This Work. Also Region of Depth Where Target is Amorphized	37

LIST OF SYMBOLS

E_0	kinetic energy of incident ion
z_1	atomic number of ion
v_0	$=e^2/h = 2.2 \times 10^8$ cm/sec
$z_1 v_0$	speed of electrons in innermost orbit of ion
v_{TF}	$= z_1^{2/3} v_0$ Thomas-Fermi velocity
R_p	the projected range in a target of incident particle
ΔR	standard deviation of projected range
S_e	electronic energy loss of ion
S_n	nuclear energy loss of ion
N_d	number of atoms displaced by incident ion
E_n	area under damage density (dv/dx) versus x curve
x	depth in solid
M_1	mass of incident ion
M_2	mass of atom in target
K	kinetic factor $= \left[\frac{M_1 \cos \theta + (M_2^2 - M_1^2 \sin^2 \theta)^{1/2}}{M_1 + M_2} \right]^2$
θ	scattering angle in laboratory system
$Y(E)$	backscattering yield
Y_A	backscattering yield in aligned direction
Y_R	backscattering yield in random direction
S	stopping power
n	ion dose, ie. number of ions/cm ²
C	heat capacity of silicon, 0.1650 cal/g K = 0.6905 j/g K
ρ	density of silicon, 2.3 g/cm ³
t	thickness of target
ΔT	temperature rise of target

SECTION I

INTRODUCTION

1. SILICON FILMS

High quality single crystal silicon films on insulating substrates are required to fabricate dielectrically isolated metal-oxide-semiconductor (MOS) devices. To achieve devices small enough for very large scale integrated (VLSI) circuits, sub-micrometer thickness silicon films are necessary. Ultimately one hopes to prepare films whose electrical properties approach those of bulk silicon. As currently fabricated, silicon films are deposited at elevated temperatures onto substrates with a coefficient of linear expansion different from that of silicon. When cooled back to room temperature, the films consequently develop strain and may exhibit twinning. Silicon-on-sapphire (SOS) is the most developed technology of the various silicon film efforts. There were some early studies on effects of defects and stress on electrical properties of the films as grown (References 1 and 2). A number of processes were developed to improve the quality of these films (References 3-16). In general these processes involve ion implantation of Si^+ into the films to create amorphous regions. Often one desires an amorphous region which comes close to the substrate-film interface but which does not disturb the interface too much. An implant which disturbs the substrate significantly can lead to serious aluminum autodoping in the case of SOS. Also, a small crystalline region at the outer surface of the film is required as a seed for the recrystallization process. By various annealing treatments, the films are then recrystallized. This may be by furnace, lamp, laser or glow bar annealing.

Theoretical calculations seldom predict the extent of amorphous regions better than a factor of two. There even seems to be some variation in the extent of amorphous regions generated by identical implanters in different locations. Thus it is necessary to know the properties of a given instrument and sample mounting arrangement before designing treatments for a given batch of films.

The main effort of this work is to describe the properties of the Air Force Wright Aeronautical Laboratories (AFWAL) Varian 400-10AR Ion Implanter owned by the

Electronic Technology Division of the Avionics Laboratory (AAD). It is operated by AADR. Its nominal operating range is from 50 keV to 380 keV. Under extreme conditions 400 keV is possible. Universal Energy Systems has a General Ionex Corporation, Newburyport, MA, 1.7 MV Tandetron accelerator. It provides 0.4 - 4.5 MeV He particles which are used in Rutherford Backscattering analysis. It can also be used as a higher energy ion implanter, normally working in the range of 400 keV to 6 MeV. However it can still operate fairly efficiently at 380 keV to provide a comparison with the Varian instrument.

The main thrust of this work is to obtain the instrumental conditions on the machines to amorphize 0.3 micron and 0.5 micron thick silicon (100) films for recrystallization. Table 1 lists the recipes reported by other workers in this field on related projects. The general consensus seems to be for 0.3 micron Si films implanted with Si^+ to use 130-200 keV ions with doses of 5×10^{14} to 2×10^{15} ions/cm² and for 0.5 micron films, 260-300 keV ions at $1-2 \times 10^{15}$ ions/cm². Svensson et al. (Reference 17) quotes an energy density criterion that 10^{21} keV/cm³ results in amorphous silicon. Thus for 0.3 micron films we obtain upper and lower limits of 13×10^{21} keV/cm³ and 2.2×10^{21} keV/cm³ — 2 to 13 times larger than the criterion. For 0.5 micron films $12-5.2 \times 10^{21}$ keV/cm³ — 5 to 12 times larger.

The difference is due, in part, to the inefficiency of the displacement process in that some atoms, although receiving sufficient energy for removal from their lattice site, relax or recombine with their original or other vacant lattice site. This effect is also temperature sensitive. Also, at these energies, only 50-70% of the energy of the implanted ions is available for the displacement process; the remainder is dissipated directly in the electronic excitation process.

2. ION IMPLANTATION

The subject of ion implantation has been covered by a number of review articles and books (Reference 18-28). To avoid channeling complications in depth ranges, we have mounted our samples on a plane whose normal is inclined 7° to the incoming beam. Also to avoid planar channeling, the silicon (100) samples were mounted at a 7° tilt with the horizontal. Thus the theory developed for a random solid should describe the situation well.

From these results it appears that the best set of values to amorphize a 0.3 micron silicon film mounted in this arrangement is 5×10^{14} ions/cm² @ 150 keV or 2×10^{14} ions/cm² @ 200 keV. For 0.5 micron Si films, it appears that a dosage greater than 5×10^{14} ions/cm² @ 200 keV or greater than 2×10^{14} ions/cm² @ 250 keV are the amorphization dosages.

On the second batch of runs on the Varian, 5×10^{14} ions/cm² @ 180 keV (Figure 7) appears to be a satisfactory combination for 0.3 micron films while 1×10^{15} ions/cm² (Figure 8) would disturb the rear interface. For 0.5 micron films, 5×10^{14} ions/cm² @ 250 keV (Figure 9) seems a bit better than 2×10^{14} . Near the substrate interface, 5×10^{14} ions/cm² @ 275 keV (Figure 10) seems a bit better than 250 keV provided enough crystal is left on the outer surface as a seed. About the same can be said for 1×10^{15} ions/cm² @ 275 keV (Figure 11) although the interface is more likely to be disturbed. Figure 12 shows that 2×10^{14} ions/cm² @ 300 keV might be used although a large amount of crystalline surface area remains. Figure 13 is the same as Figure 12 followed by a 2×10^{14} ions/cm² dose @ 120 keV. Note that most of the region out to the surface is now amorphized. Dosages of 5×10^{14} ions/cm² @ 300 keV (Figure 14) and 1×10^{15} ions/cm² @ 325 keV (Figure 15) would destroy the interface at a 500 nm depth (0.5 micron).

Several samples were run on the Tandetron implanter at UES with the samples essentially suspended in free space. Figure 16 shows the results of 1×10^{15} ions/cm² @ 180 keV. This should be compared with Figure 8. The two traces are relatively similar with the UES sample showing more crystalline regions at the surface and the amorphous region extending only 300 nm deep instead of 350 nm. Figures 9 and 17 exhibit dosages of 5×10^{14} ions/cm² @ 250 keV. These exhibit drastic differences. The UES sample is amorphous (maybe never totally amorphous) only between 220 and 290 nm, while the sample on the LN₂ dewar is amorphous between 10 and 380 nm. Figures 12 and 18 show dosages of 2×10^{14} ions/cm² @ 300 keV. Here the UES sample never really shows an amorphous region. Figures 14 and 19 display dosages of 5×10^{14} ions/cm² @ 300 keV. Both have roughly the same shape with the cooled sample approaching the random spectrum a bit more. Thus there seem to be considerable differences between the results on some of these samples. Experimentally the major difference seems to be the temperature of the target.

To resolve some of these discrepancies, a third batch of samples were run on the Varian instrument. This time the dewar was left at room temperature. Two samples

Aligned yield after implantation with 250 keV silicon to the doses indicated

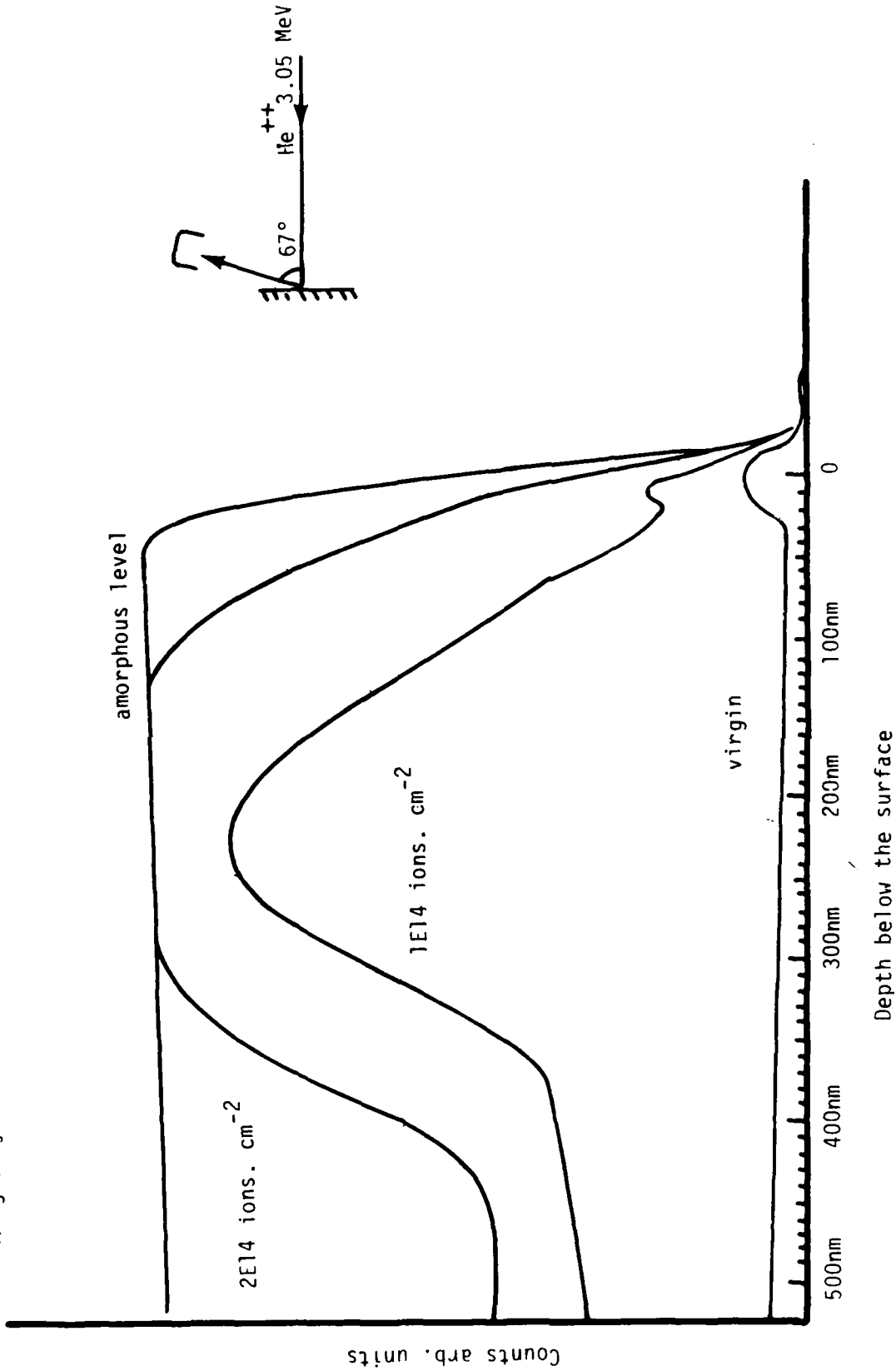


Figure 6. Si Into Si Implants Using Varian Machine. 250 keV Incident Ion Energy at $1 \text{ \& } 2 \times 10^{14} \text{ Ions/cm}^2$. LN_2 in Dewar

Aligned yield after implantation with 200 keV silicon to the doses indicated

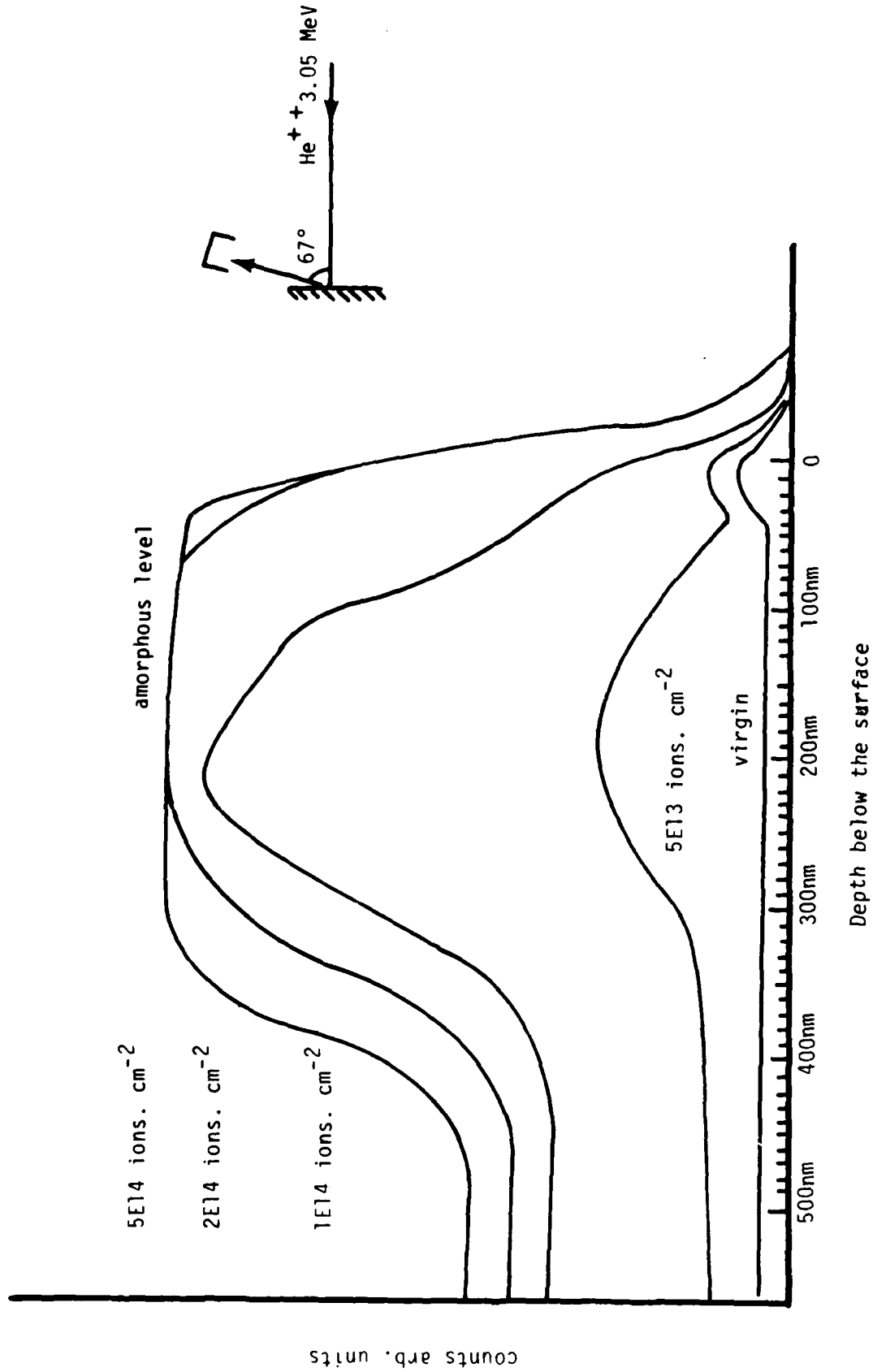


Figure 5. Si Into Si Implants Using Varian Machine. 200 keV Incident Ion Energy at 0.5, 1, 2, & 5×10^{14} Ions/cm². LN₂ in Dewar

Aligned yield after implanatation with 150 keV silicon to the doses indicated

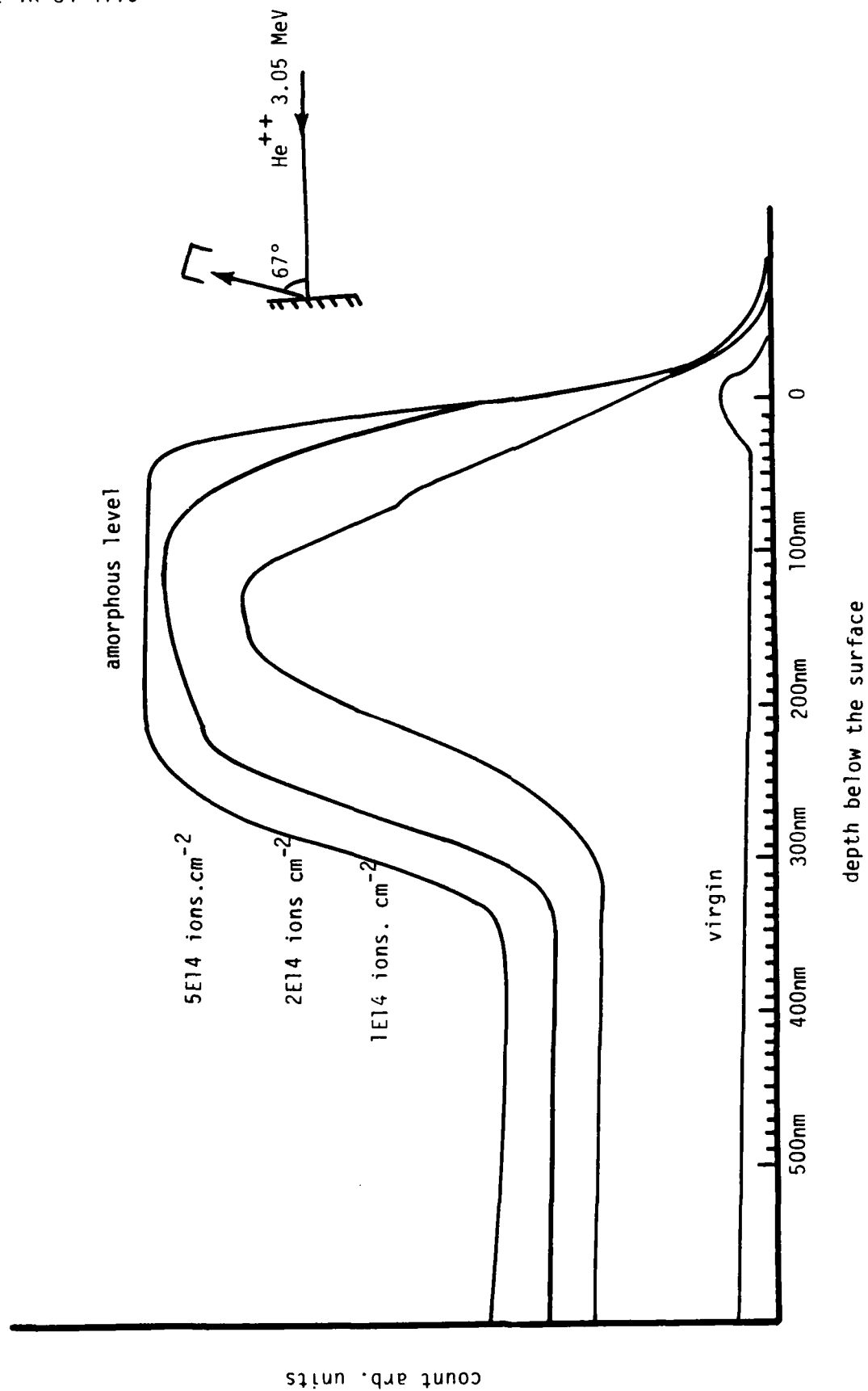


Figure 4. Si Into Si Implants Using Varian Machine. 150 keV Incident Ion Energy at 1, 2 & 5 X 10¹⁴ Ions/cm² Doses. LN₂ in Dewar

SECTION II

EXPERIMENTAL WORK

As stated in the introduction, the purpose of this work was to ascertain the experimental conditions to amorphize 0.3 and 0.5 micron thick silicon (100) films for recrystallization using two implanters located in Dayton, Ohio. One desires a small crystalline region on the surface to serve as a seed in the recrystallization process. Also one does not wish to disturb the interface between the film and the substrate since this would tend to introduce impurities into the film from the substrate.

The samples implanted by the Avionics Laboratory implanter were (100) bulk silicon which was n-type due to P doping. They were 12 mm x 12 mm x 0.5 mm squares, cut from 2 inch diameter silicon wafers. The samples run on the UES machine were (111) silicon. The results should be comparable since the samples were oriented to appear like a random lattice target to the incoming ion beam.

At the Avionics machine the samples were mounted horizontally off by about 7°. The target block which incorporates a dewar was then rotated to be 7° off the normal to the beam. Thus axial and planar channeling were avoided. Half the sample was covered with aluminum foil. Thus half the sample was undamaged. In this portion the optimal channeling direction could be obtained in Rutherford backscattering measurements, then the sample could be translated sideways and the spectrum in that direction in the damaged part of the crystal could be obtained.

Most samples were attached to the stainless steel dewar mounting block by glueing them on with rubber cement. Thus there was considerable thermal isolation between the sample and the dewar. The temperature of the sample was probably significantly different from that of the dewar, especially for high energy and/or high dosage runs. The first batch of samples on the Varian instrument were run at room temperature and were not half covered by aluminum foil. It was almost impossible to determine a channeling direction on them, so further analysis on them was abandoned. The second batch of samples on the Varian were half covered with aluminum foil and the dewar filled with liquid nitrogen. Various dosages were obtained with 150, 200 and 250 keV energy Si^{+28} implants. See Figures 4, 5, and 6.

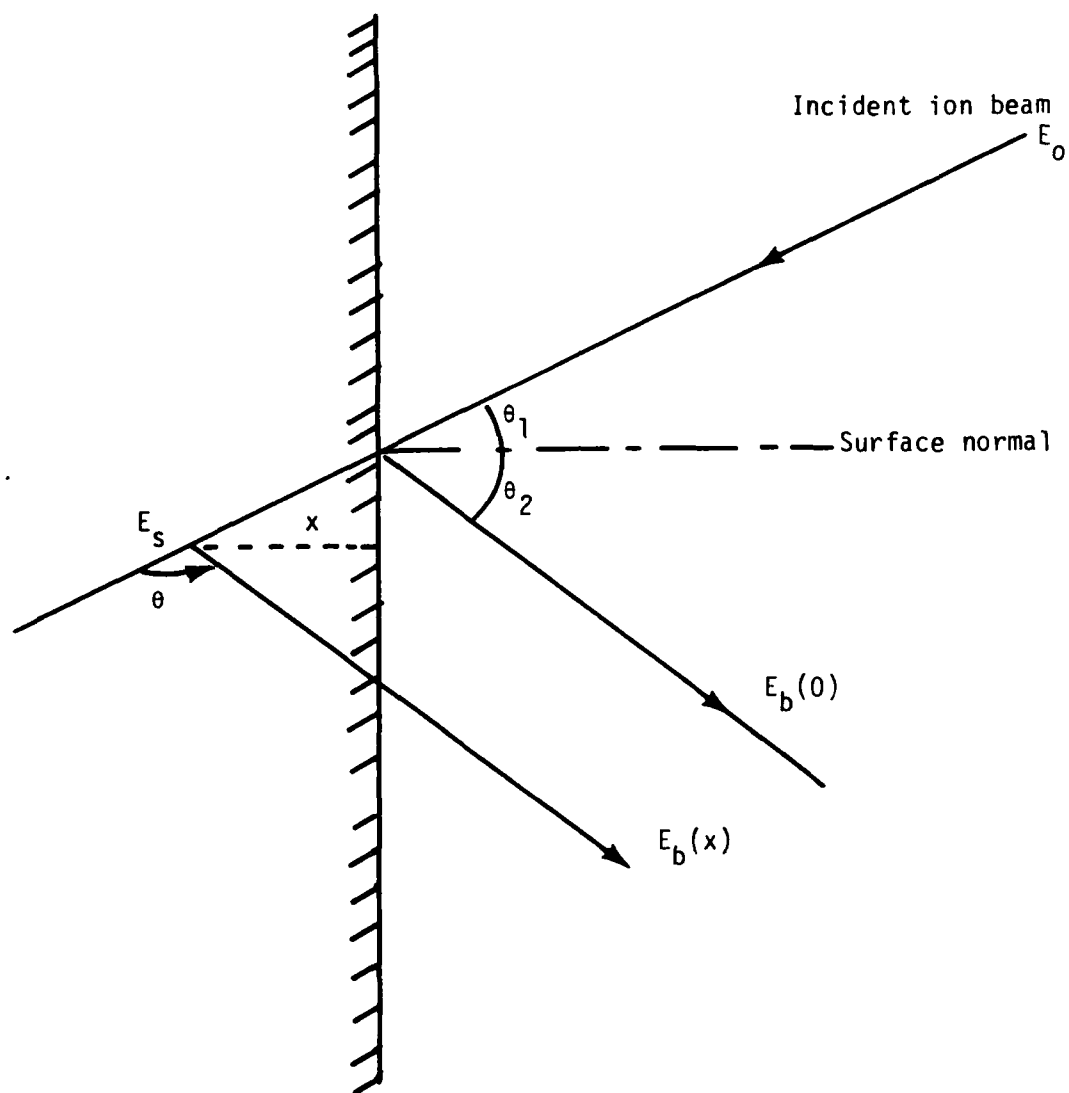


Figure 3. Definition of Angles and Depths in Rutherford Backscattering Measurements

spectrum, one measures the yield. The fraction that it is to the random beam, $\chi(x) = Y_A(x)/Y_R(x)$ at equal depths, can be used as a measure of the quality of the single crystal. If the crystal has been damaged by a previous implant, the actual observed spectrum lies between the two extremes. If half the sample is covered with aluminum foil during the silicon implant, then the sample can be oriented along a channeling direction using the undamaged part of the crystal. Next, the crystal is translated in the channeling orientation and a spectrum of the damaged part of the crystal is obtained with some confidence that the orientation is proper. Thus, one can compare the channeled spectrum in the undamaged part of the crystal, which provides a measure of the original crystal quality, with the damaged region and the random spectrum.

One other problem is to convert the energy scale into a depth scale from the surface of the target. See Figure 3. E_0 is the incoming beam energy. $E_b(x)$ is the beam energy at the detector of particles scattered at x . Assume a constant stopping power for the ingoing path, $S(E_0)$, and a constant stopping power for the outgoing path, $S(KE_s)$. The energy difference between particles scattered at the surface and at a depth x is

$$E_0 - E_b(x) = x \left\{ \frac{KS(E_0)}{\cos\theta_1} + \frac{S(KE_s)}{\cos\theta_2} \right\}$$

So any measured energy difference can be converted into a depth, if reliable values of S are available from tables.

The depth scale that is drawn on the spectra shown in the experimental section is generated with the RBS simulation computer program which we obtained from Agronne National Laboratory. The zero for the depth scale corresponds to scattering from the surface. The energy for scattering from the surface is $E_s = K_m E_0$ where E_0 is the incident energy and K_m is the kinematic factor for Si with the detector at 105° . Using the simulation program, the energy of a He ion scattered from a depth of 100, 200, 300, and 400 nm can be obtained. In the case of 100 nm, the computer code uses 40, 2.5 nm thick layers to compose the 100 nm layer. The stopping power is calculated for each layer. The computer code generates a spectrum on the display. From the display the energy for scattering from 100 nm can be obtained.

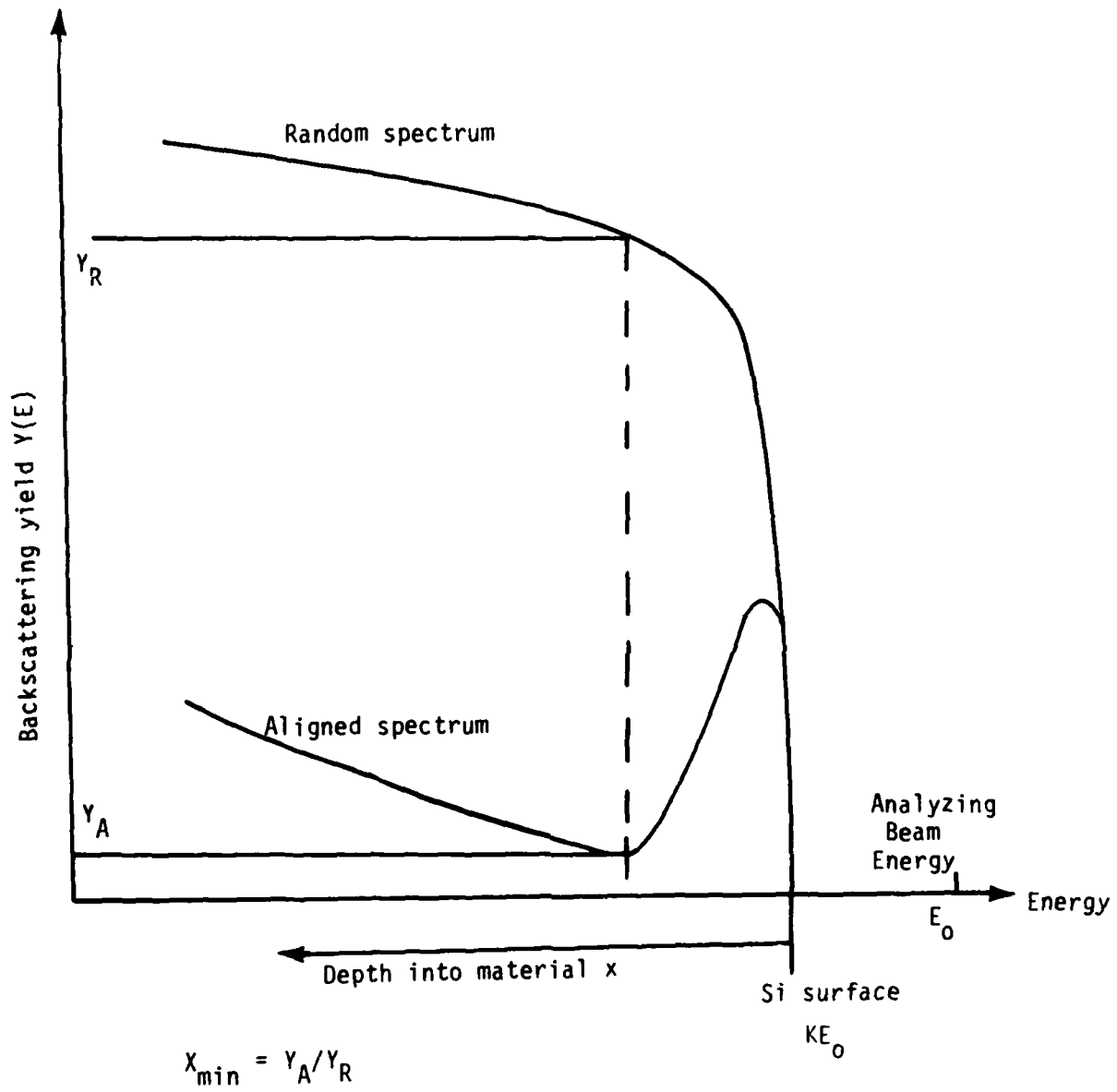


Figure 2. Schematic Rutherford Backscattering Yield Plots for Random and Aligned Directions Versus Energy

final fate at times greater than 10^{-9} seconds after the impinging ion has come to rest. Thus any displaced atoms which relax back onto a lattice site or are able to diffuse to a vacant lattice site will not be among those which remain displaced. Such effects can reduce the displacement efficiency by an order of magnitude (Reference 37) (p.169 of Reference 27). Thus a critical parameter is the temperature of the sample during implantation.

According to the model of Morehead and Crowder (Reference 37), the major factors for the formation of a continuous amorphous layer are the ion mass, dose and target temperature. Some less important variables are dose rate and ion energy. However if the layer is desired at a specified depth and width in the sample, the ion energy takes on major importance.

4. RUTHERFORD BACKSCATTERING AND CHANNELING

The experimental technique used to characterize the amorphous region is Rutherford backscattering channeling (References 27 and 38). A beam of high energy light particles, usually 1-2 MeV He^+ , hits the target mounted on a goniometer located inside a vacuum system. After striking the target some of the beam is scattered and is detected by a solid state detector within a given solid angle as a series of pulses. The height of the pulses depends on the energy of the particle entering the detector. After a period of time, the output of a multichannel analyzer looks something like that shown in Figure 2. The energy of a particle of mass M_1 , energy E_0 , scattering from a particle of mass M_2 at the surface of the target is $E = K E_0$,

$$\text{where } K = \left[\frac{M_1 \cos \theta + (M_2^2 - M_1^2 \sin^2 \theta)^{1/2}}{M_1 + M_2} \right]^2 \quad \text{and } \theta \text{ is the scattering angle in the laboratory system.}$$

For He^+ scattering from Si at $\theta = 113^\circ$, $K = 0.840$, for $M_1 = 4$, $M_2 = 28$. $M_2^2 = 784$ and $M_1^2 = 16$, so that the above expression can be approximated as

$$K = \left[\frac{M_1 \cos \theta + M_2}{M_1 + M_2} \right]^2 = 0.857$$

A typical amorphous or randomly excited single crystal spectrum is shown in Figure 2. (See e.g. Reference 27, esp. pp. 87-93). If a crystal is oriented so that one is along a channeling direction, a spectrum as shown is obtained. The yield never reaches zero since there will always be scattering from the ends of close packed rows of atoms in the target. At the minimum of the yield in the aligned

3. DAMAGE DISTRIBUTION AND ATOMIC DISPLACEMENT DUE TO ION IMPLANTATION

As an implanted ion traverses into a target, it loses energy via collisions until it is stopped. An individual ion tends to produce a damage cluster region roughly in the shape of a cylinder. In many cases enough energy is imparted to target atoms to displace them from their initial location. Sometimes enough energy is imparted to permanently displace them, and other times they are displaced only for a given period of time. These damage clusters and their interaction promotes the crystalline-to-amorphous transition in regions of the target. The theoretical work of Kinchin and Pease (Reference 34) provides a framework to analyze data. Their estimate for the number of atoms displaced by the "average" ion is $N_d = E_n/2E_d$, where E_n is the area under the damage density ($d\bar{v}/dx$) versus x , depth in solid, curve. E_d is the displacement energy for a target atom. For almost all solids and implant orientations, it is within an order of magnitude of 15 eV.

The heat generated by the implantation process tends to promote atoms hopping in to heal much of the damage generated in some sort of healing process. Thus, targets which are cooled tend to have deeper and more pronounced amorphous regions. Hence in characterizing the amorphous region generated, the substrate temperature is an important quantity along with the implanted ion's energy and dose.

Reference 27 has an extended discussion on damage and the creation of amorphous regions in its Chapter 5, especially pp. 124-138. In all cases discussed, plots of disorder, D , depth profiles have roughly the same shape as the calculated range, R , but always have a peak occurring nearer the surface of the target than the peak in the the range. Experiments indicate that in Si about twice as many defects are generated than predicted by theory. In GaAs the measured number of defects is less than predicted by theory.

Crowder and Title (Reference 35) made a study of the peak in the damage of the silicon lattice with respect to the peak of the ion depth distribution. All these studies used incident energies below 300 keV and dosages of 10^{12} - 10^{14} ions/cm². For Si²⁹ with 150 keV energy at 2×10^{13} ions/dm² dose, the damage peak was 140 nm while the ion peak was at 220 nm. The ratio of these distances was 0.6. All the ions studied had a ratio in the 0.5 to 0.7 range.

The Kinchin and Pease model (Reference 34), and the variants thereto (Reference 36) only consider the displacement of atoms. They are not concerned with their

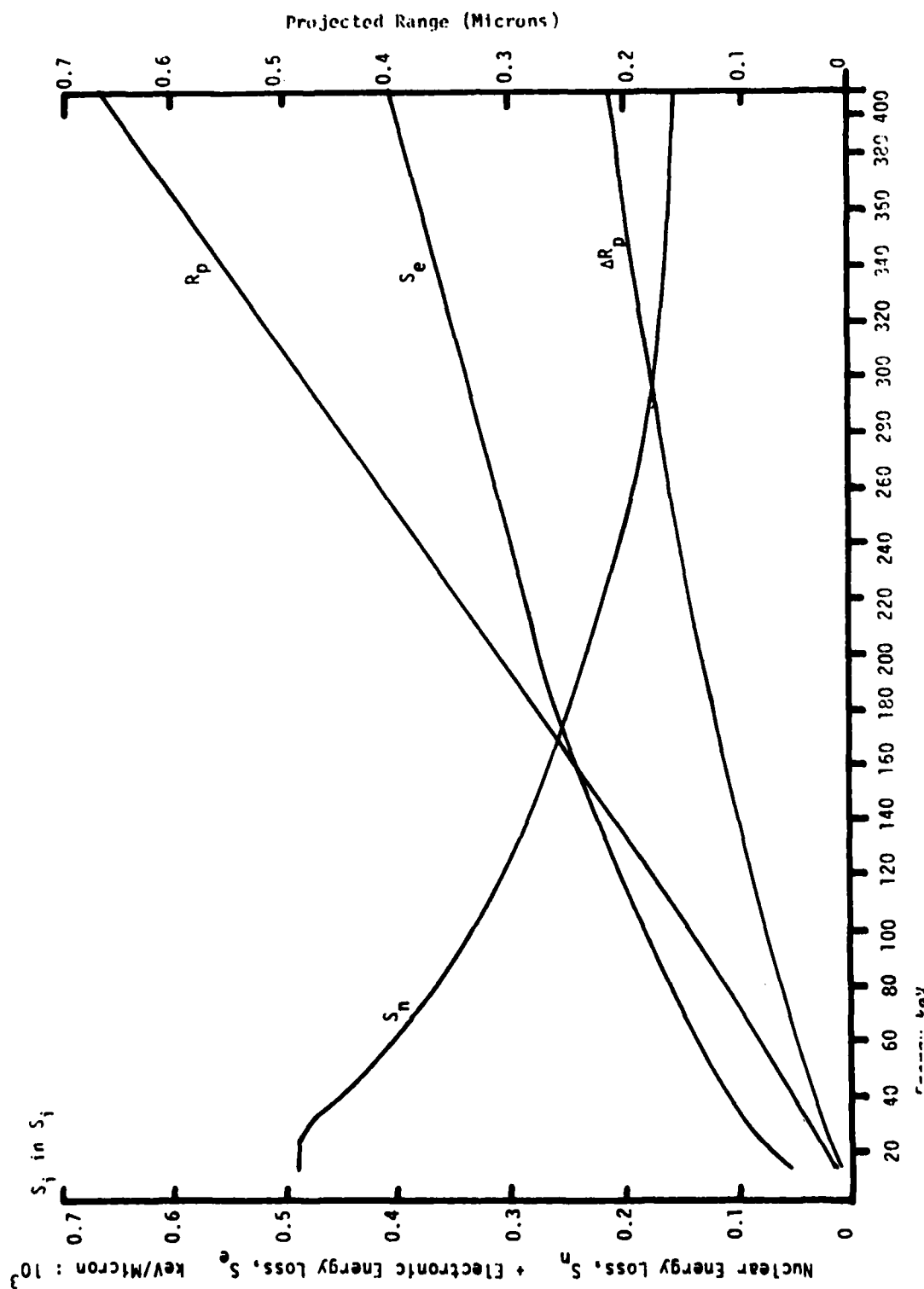


Figure 1. Plots of Nuclear Energy Loss S_n , Electronic Energy Loss S_e , and Projected Range R_p for Si into Si taken from B. Smith Ion Implantation Range Data for Silicon and Germanium Device Technology

The implanted ion loses energy to atoms in the target by two independent processes, namely nuclear (elastic) and electronic (inelastic) collisions. The relative importance of these two energy-loss mechanisms varies with the kinetic energy E_0 and the atomic number z_1 of the bombarding particles. Nuclear stopping predominates for low E and high z_1 ; electronic stopping predominates for high E_0 and low z_1 . As long as the velocity of the particle in matter is large compared with the speed $z_1 v_0$ ($v_0 = e^2/h = 2.2 \times 10^8$ cm/sec) of its electrons in the innermost orbit, the particle is stripped of its electrons and moves as an ion through the target. The maximum of the stopping power curve usually lies a bit above the Thomas-Fermi velocity, $v_{TF} = z_1^{2/3} v_0$. This value can be used to separate which loss regime predominates. For silicon with $z_1=14$ and $M=28$ amu, we have $v_{TF}=12.8 \times 10^8$ cm/sec and $E = 2.37$ MeV. Thus according to this analysis, almost all energy loss in our experiments, where E was never above 380 keV incident energy, is due to nuclear collisions. However, as we shall see, this rough estimate sets the cut off about an order of magnitude too high.

Several books of tables of ion implantation range data are available (References 29-32). We shall follow the results in the book by Bernard Smith (Reference 32). He calculates the distance a particle travels in from the surface to where it stops, R_p , the projected range. As a first approximation, one assumes that the final spatial resolution is Gaussian with a standard deviation in range ΔR . The tables are obtained by solving the range distribution equations of Lindhard, Scharff and Schiott (LSS) (Reference 33). A fundamental assumption of the LSS theory is that the target is amorphous. Thus our choice of orienting the sample closely approximates that situation. The low energy section of the energy loss versus ion energy follows the relationship, $S_e = k E^p$.

For Si into Si, from Table 1 of page xi in Smith's tables (Reference 32), $k = 3.01 \times 10^{-15}$ eVcm²/keV^p and $p = 0.55$. Figure 1 shows plots of values in Smith's tables for Si into Si over the energy range available to us. From them we see that the stopping power of S_e and S_n are equal in magnitude at 170 keV, a much lower value than the estimate in the previous paragraph. In many situations in ion implantation, calculations can only give an order of magnitude result. Thus for precise work, it is necessary to measure the quantities experimentally on standard samples for various experimental conditions, e.g. target temperature.

TABLE 1 (Concluded)

			DOSE	ANGLE		
Hewlett-Packard	0.2 μm (100) Si on (1102)	130	10	0°	960°C for 2 hours in H ₂ atmosphere removes 500Å of Si etch in HCl in H ₂ , remove another 600-800Å last of top used as seed material grow an additional 0.45-0.55 μm epitaxial Si	12
"	"	0.3-0.67 μm (100) Si on (1102)	200 300 400 500	10	0° 550°C-950°C for about 2 hours typical flux 10 ¹⁵ ions/cm ² sec 950°C gave better Xtal	13
"	"	(001) Si on (1102)	① less than 250 nm Si on substrate @ 960°C ② 55-130keV implant 10 ¹⁵ cm ⁻² ③ etch off 50-100 nm with HCl in H ₂ CVD deposit 450-550 nm Si			14
Naval Ocean Systems Command	0.45-0.8 μm (100) Si films	265	10-20		120 min @ 540°C then 60 min @ 950°C	15
"	"	0.3 μm Si	① 150,170 or 190	10	2 step anneal ① 3 hours @ 550°C ② 1 hour @ 1050°C in flowing N ₂	16
			② 100	20	① 3 hrs @ 550°C ② 3 hrs @ 550°C 72 hrs @ 1050°C	
Chalmers U.	1 μm (100) Si on (1102)	300	RT	10	7° ion beam annealing @200°C and 300°C with 300 keV ²⁰ Ne ⁺ 7.5x10 ¹³ - 1.0x10 ¹⁶ ions/cm ² rate 3x10 ¹² ions/cm ² s	17

TABLE 1

SUMMARY OF SOS RECRYSTALLIZATION USING Si⁺
IMPLANTATION AND HEAT TREATMENTS

GROUP	Si FILM THICKNESS & ORIENTATION	ION ENERGY in keV	TARGET TEMPERATURE	DOSE 10 ¹⁴ ions/cm ²	ANGLE	HEAT TREATMENT furnace anneal unless stated otherwise	REFERENCE
Mayer	0.6 μm (100) on (1102)	80-550	LN ₂	3-10	7°	550°C for 70 min	3
Golecki	0.6 μm	550 360 450	-70°C RT	7 3 20	<1° <1°	560°C in vacuo or flowing Helium	4
"	0.2 - 0.5 μm (100) CVD Si on (1102)	170 (0.2 μm) 360 (0.4 μm)	25°C 25°C	10 17	7° 7°	578°C in vacuo 40 min & cw Ar laser $\lambda = 0.5 \mu\text{m}$ 7.5W @ 15cm/s	5
"	0.41-0.47 μm (100) Si on (1102)	350 350	-170°C LN ₂	5 10	30° 0 or 7°	540-575°C in vacuo	6
"	0.37 μm (100) Si on (0112)	300	RT	16	0°	cw Ar laser, $\lambda = 0.5 \mu\text{m}$ 7W 5 & 15 cm/s	7
"	0.2 μm (100) Si on (0112)	(1) 160 (3) 80		13 20	(2) 560°C for 40min (4) 567°C for 102min		8
Toshiba	0.3 μm (100) on (1012)	190		10		1000°C for 20 min in N ₂ regrow surface subsequent 1000°C anneal	9
"	0.3 μm	(1) 190 (2) 100	amorphize Si-sapphire interface amorphize Si surface	10 20		1000°C for 20 min N ₂ ambient second anneal	10
"	0.185 μm Si (100) on (1102)	120	liquid freon	4-300		isothermal anneal @ 600°C 10-40 min also 1000°C some at 60min 1 hour 900°C, 1000°C & 1100°C	11
	0.3 μm	200		"			

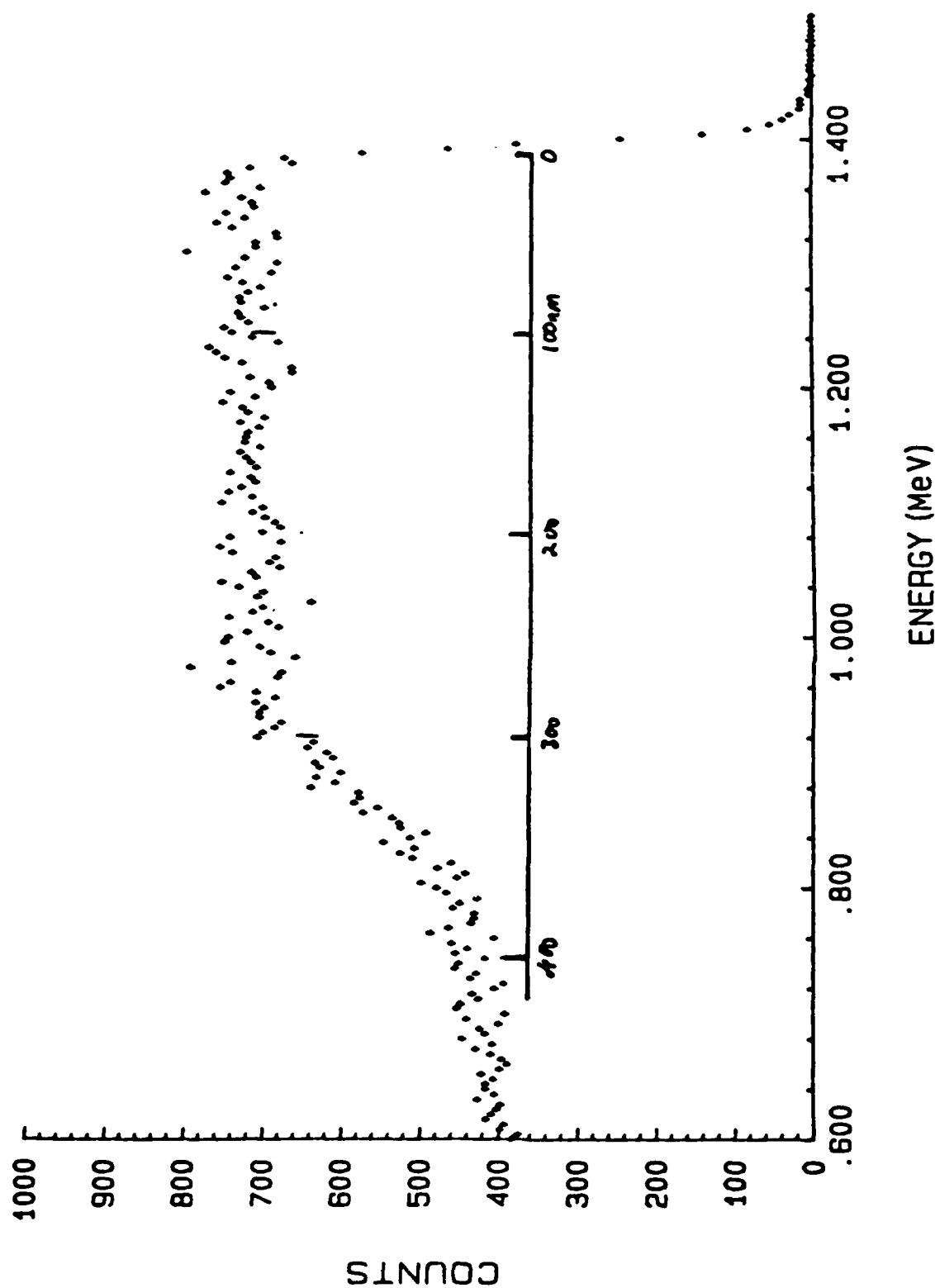


Figure 7. Si Into Si Implants Using Varian Machine. $180 \text{ keV @ } 5 \times 10^{14} \text{ Ions/cm}^2$
 LN_2 in Dewar

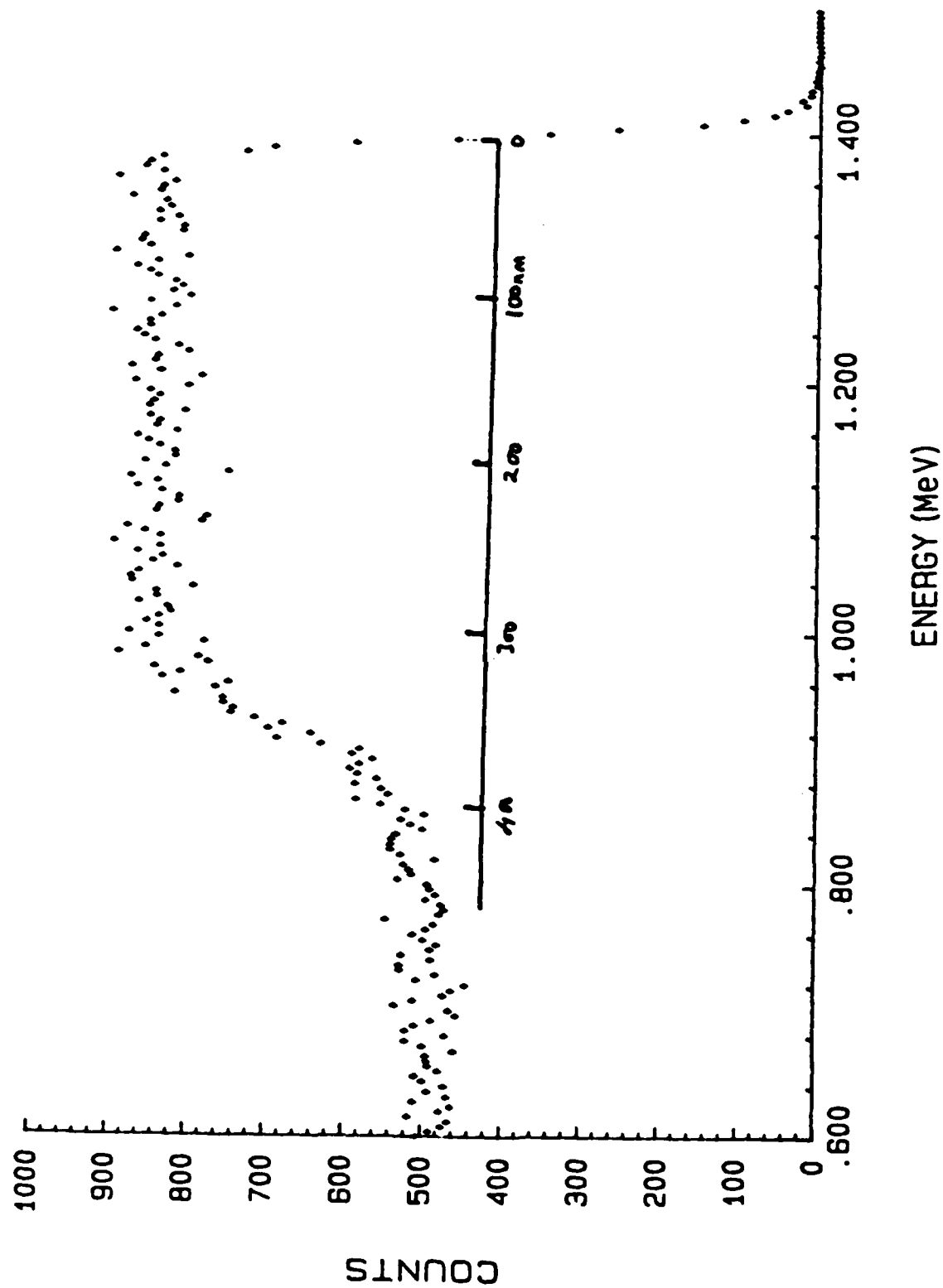


Figure 8. Si Into Si Using Varian Machine. 180 keV @ 1×10^{15} Ions/cm². LN₂

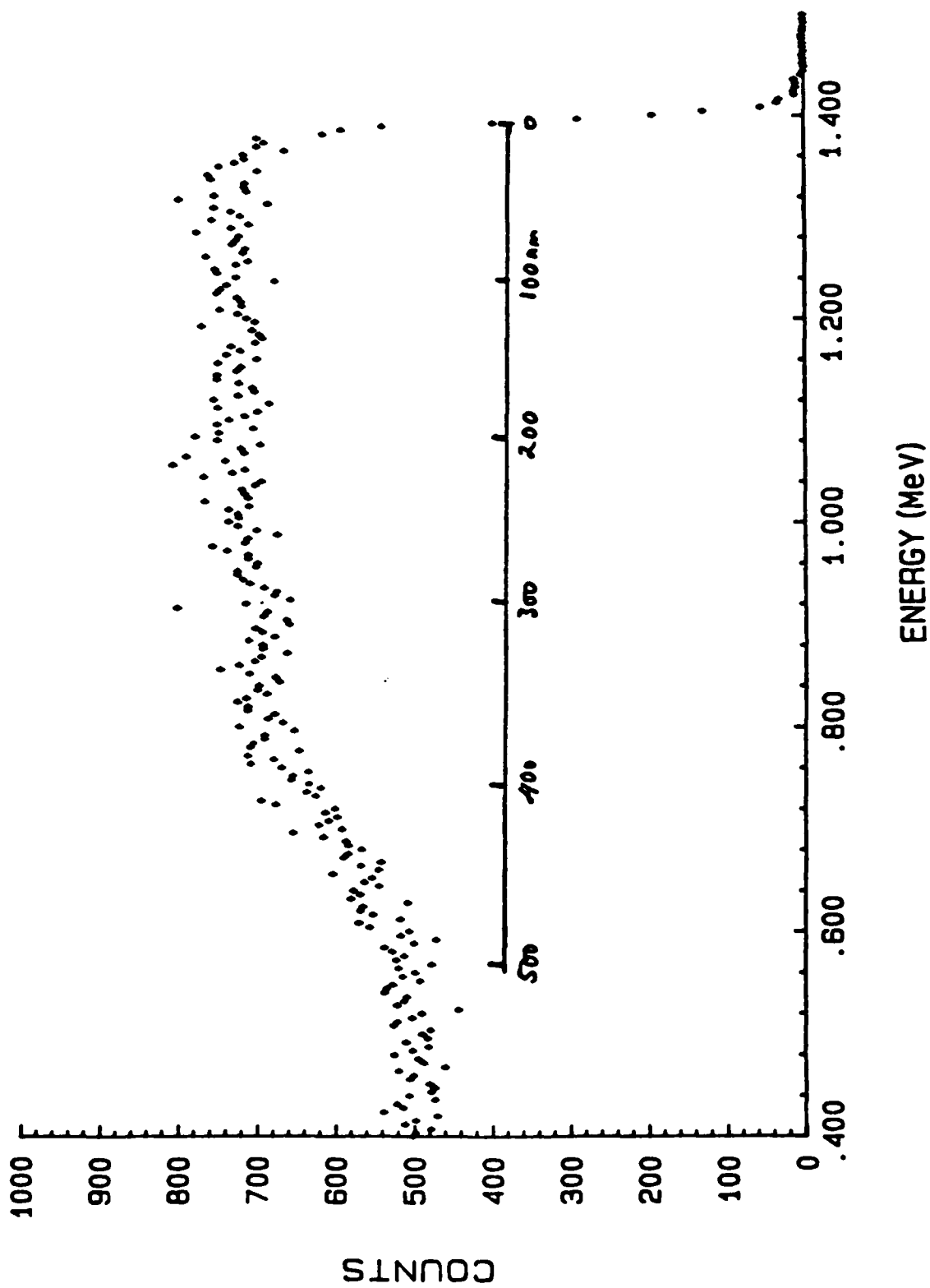


Figure 9. Si Into Si On Varian Machine. 250 keV @ 5×10^{14} Ions/cm². LN₂ in Dewar

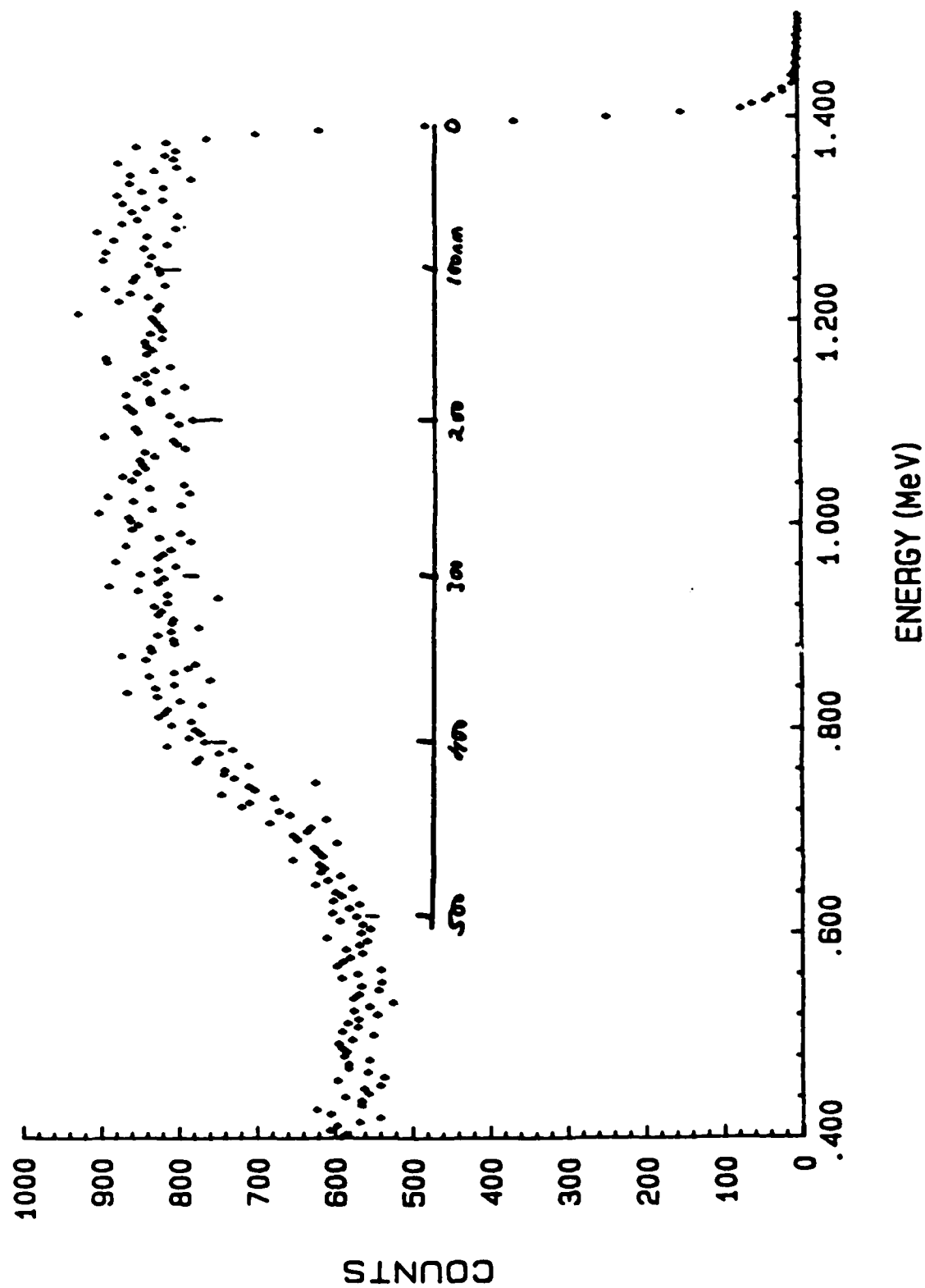


Figure 10. Si Into Si On Varian Machine. $275 \text{ keV} @ 5 \times 10^{14} \text{ Ions/cm}^2 \text{ LN}_2$

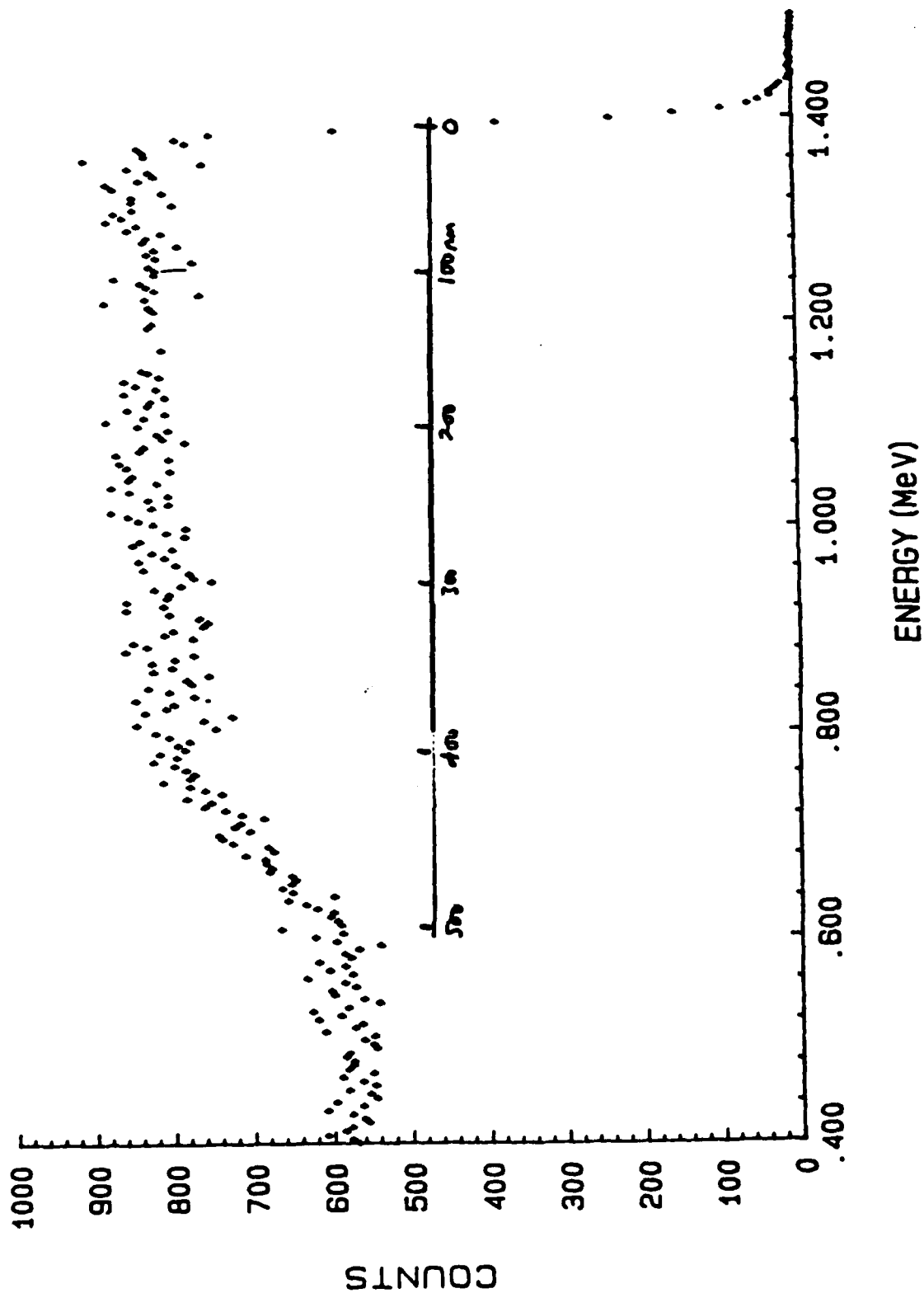


Figure 11. Si Into Si On Varian Machine. 275 keV @ 1×10^{15} Ions/cm² LN₂

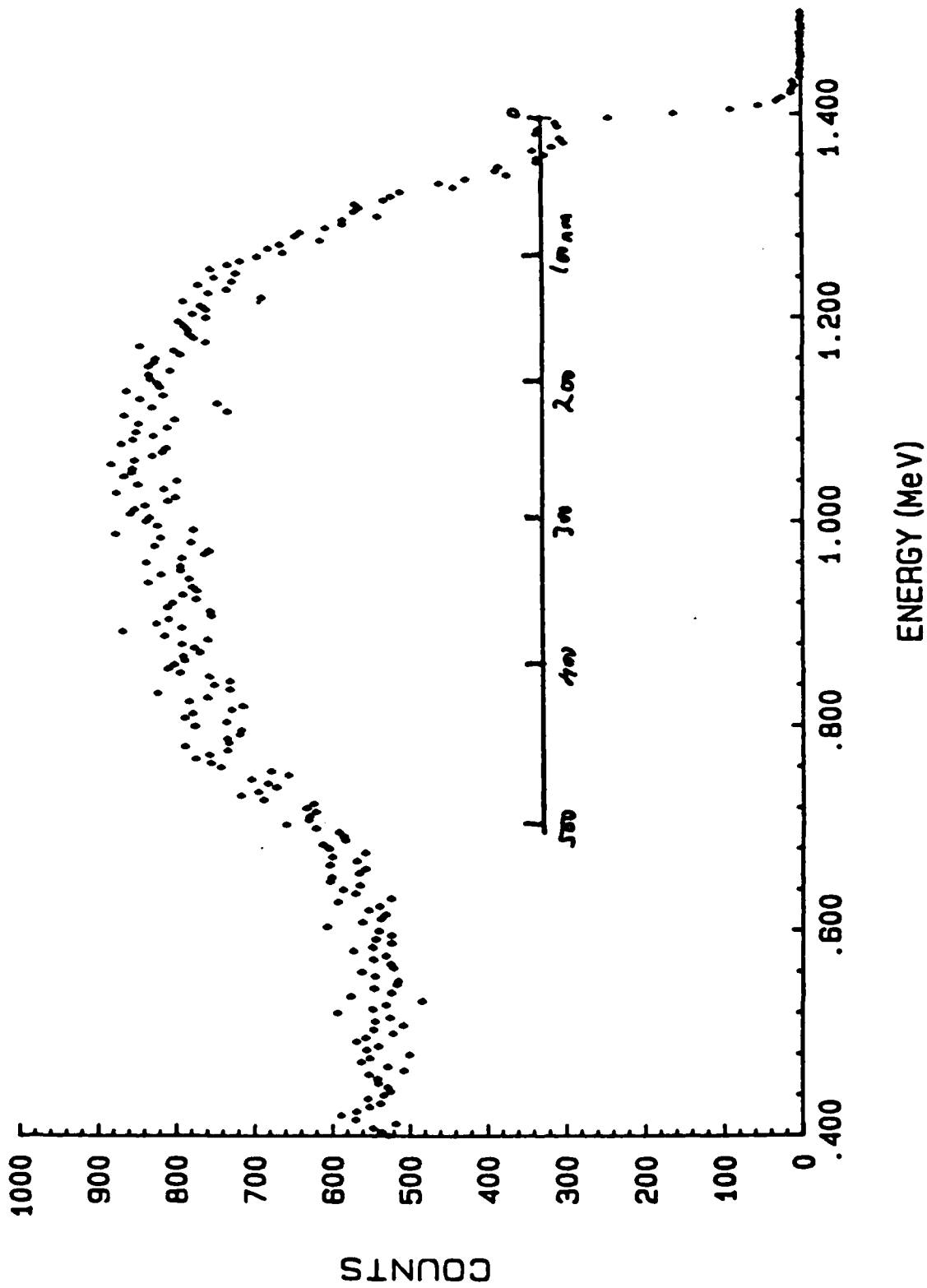


Figure 12. Si Into Si On Varian Machine. 300 keV @ 2×10^{14} Ions/cm² LN₂

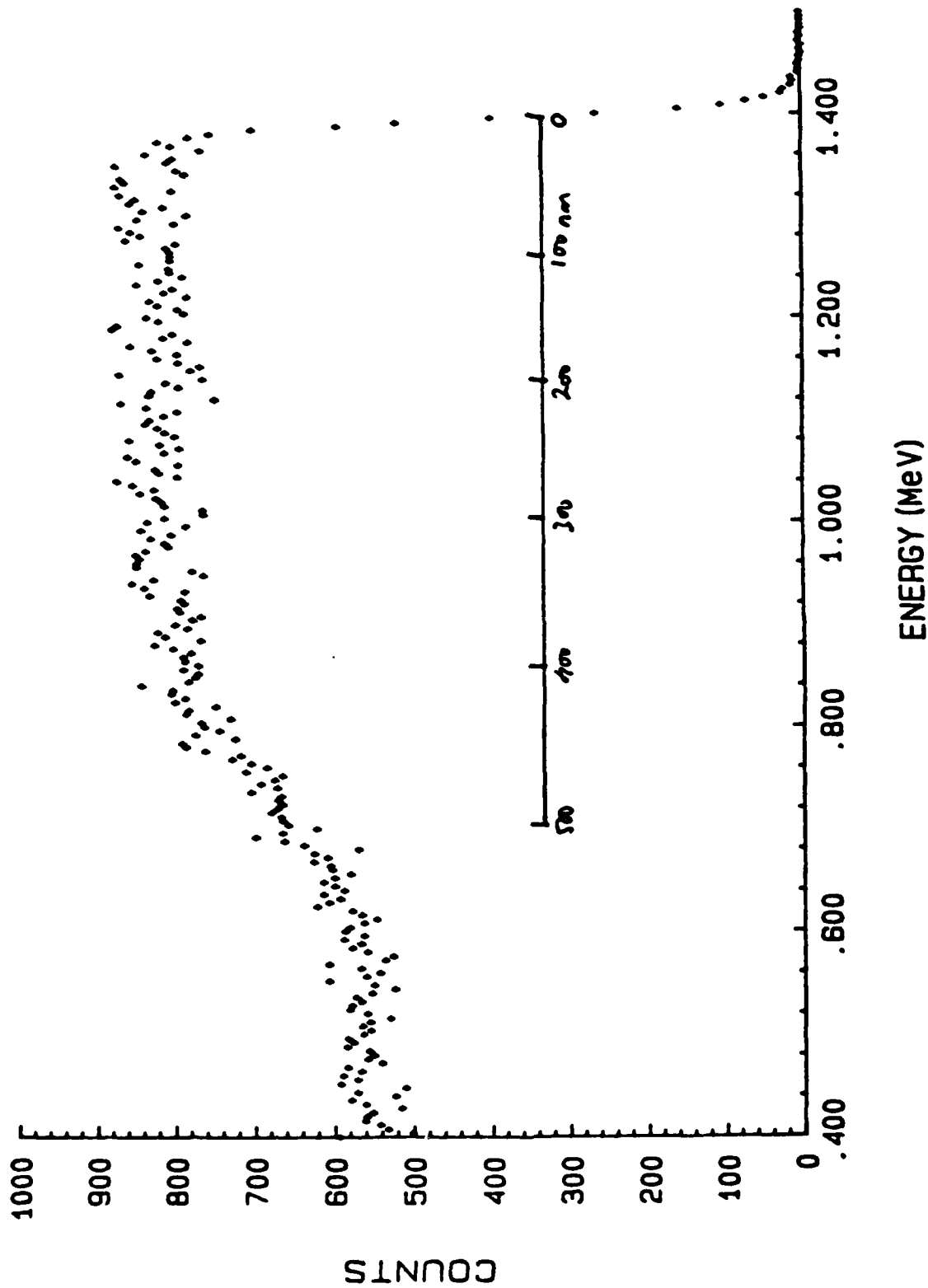


Figure 13. Si Into Si on Varian Machine. $300 \text{ keV @ } 2 \times 10^{14} / 2 \times 10^{14} \text{ Ions/cm}^2$
 LN_2 in Dewar

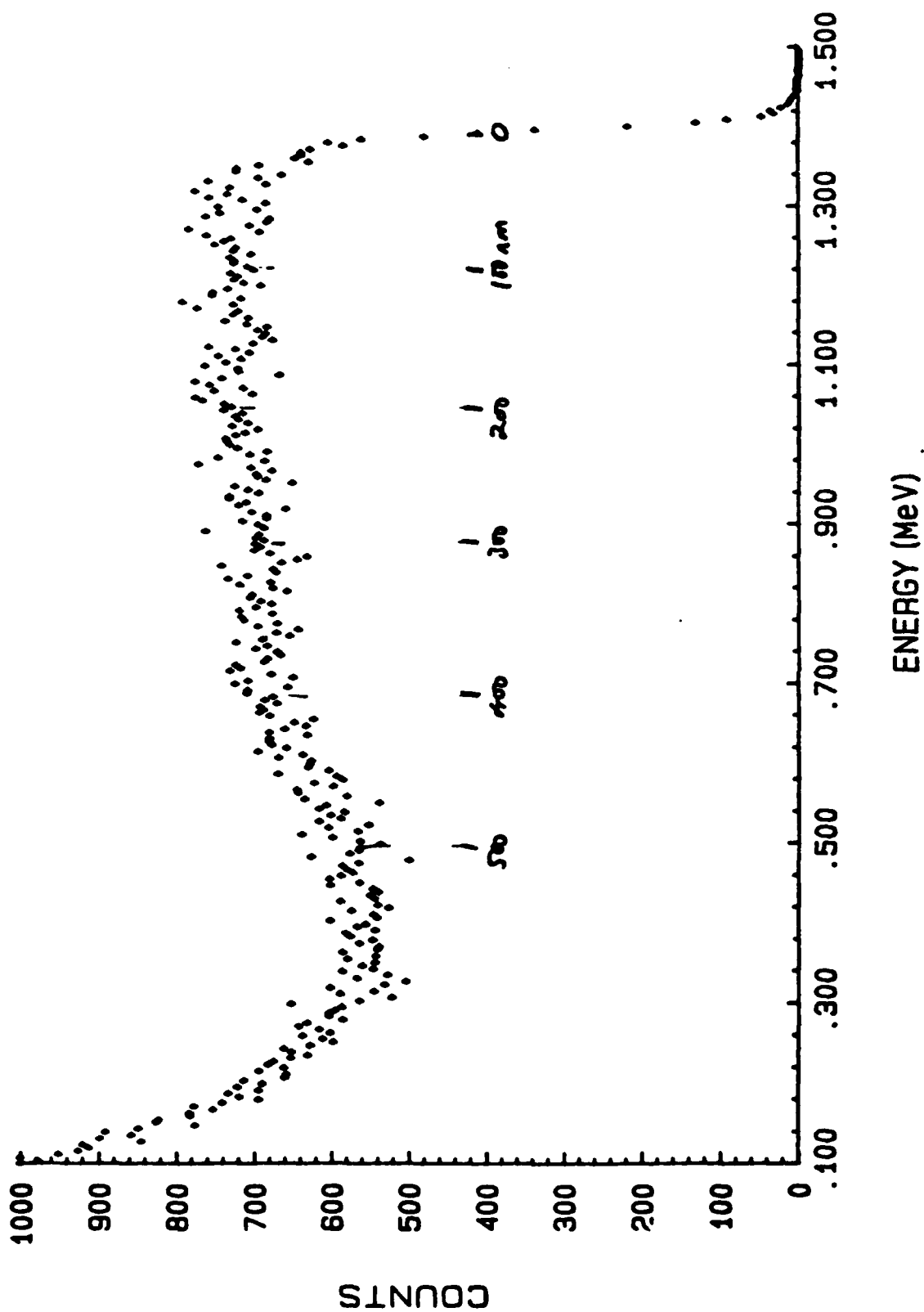


Figure 14. Si Into Si On Varian Machine. 300 keV @ 5×10^{14} Ions/cm² LN₂

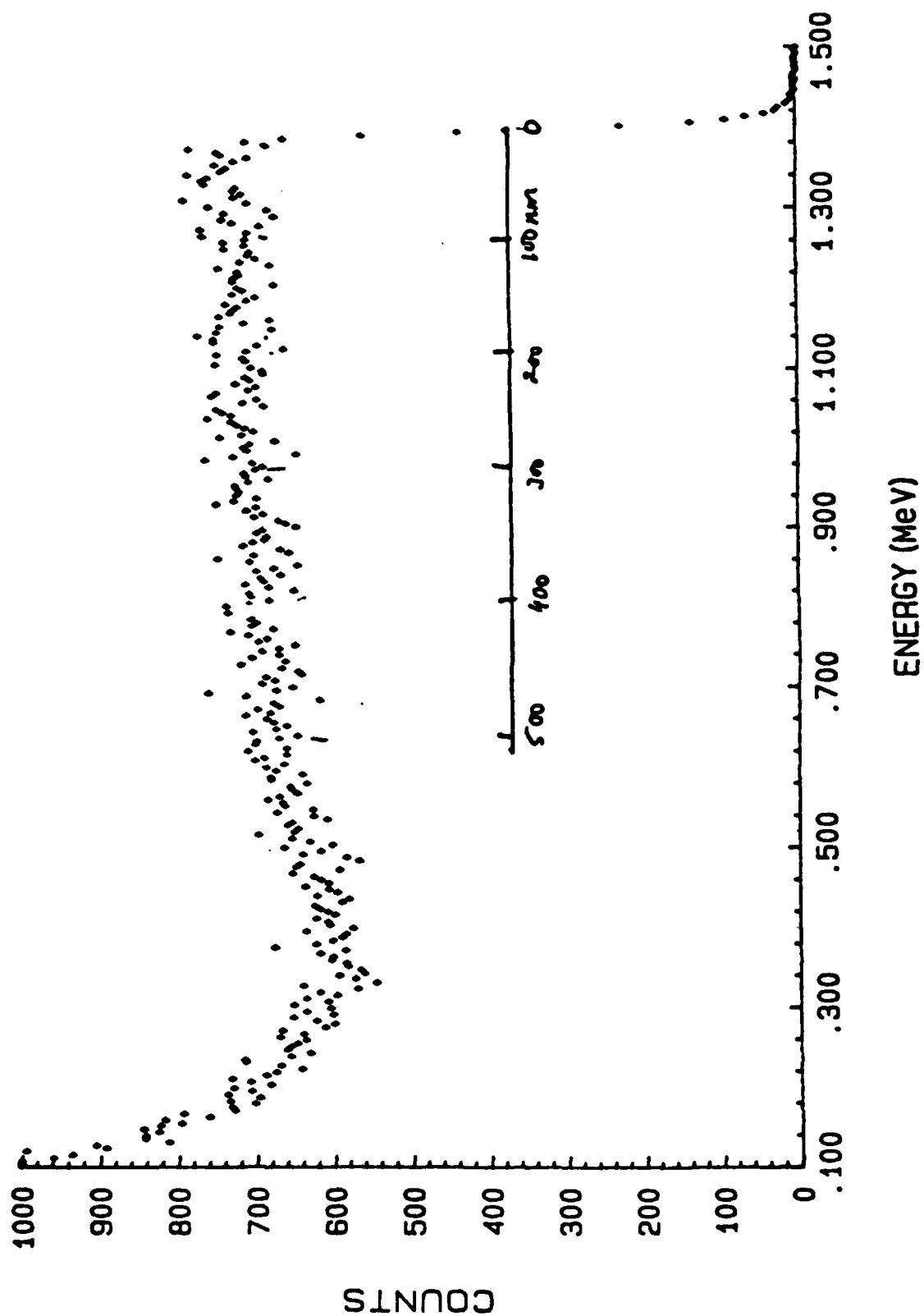


Figure 15. Si Into Si On Varian Machine. 325 keV @ 1×10^{15} Ions/cm² LN₂

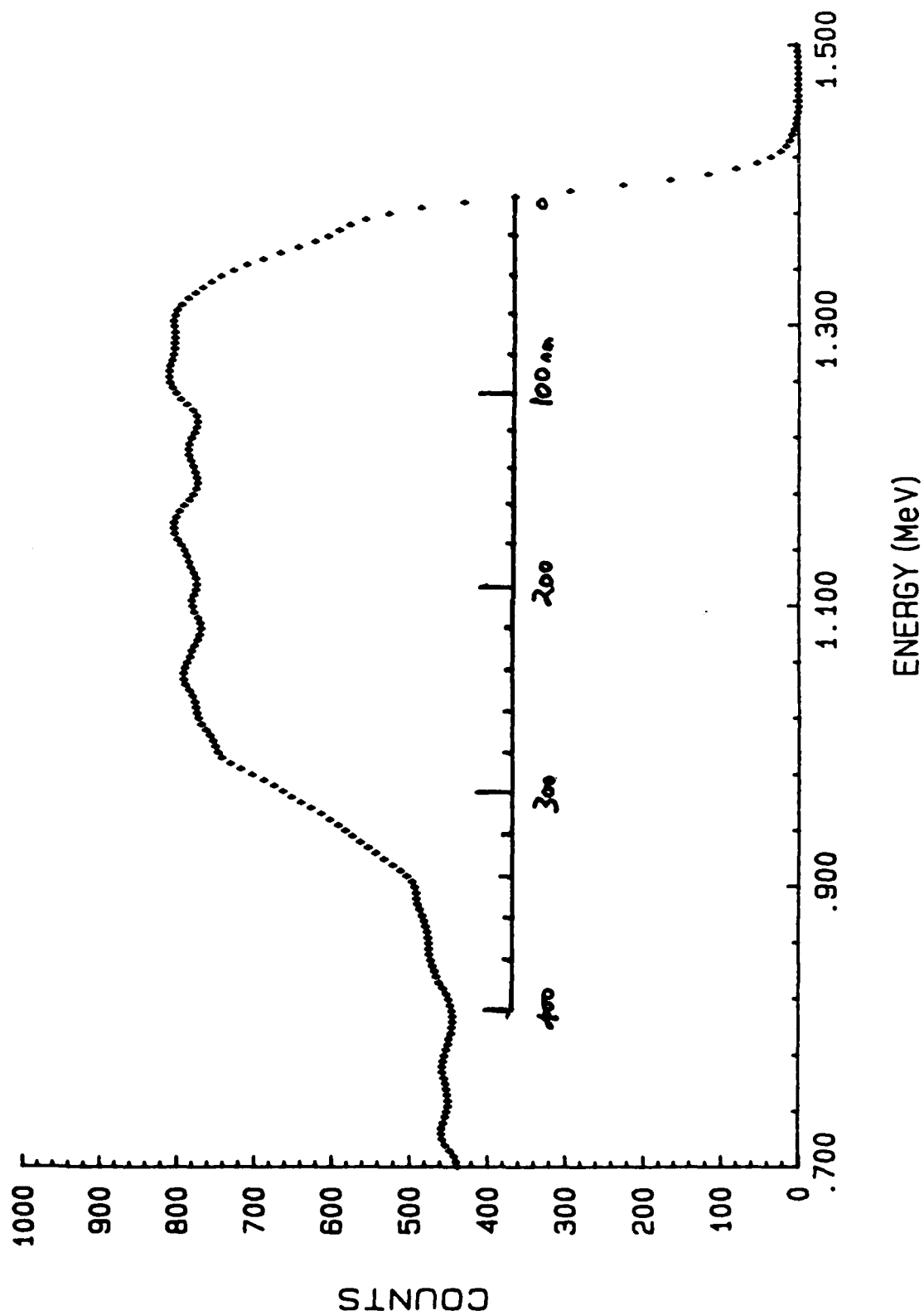


Figure 16. Si/Into Si Using Tandetron. 180 keV Incident Ion Beam Energy With 1×10^{15} Ions/cm² Dose. Initially at Room Temperature

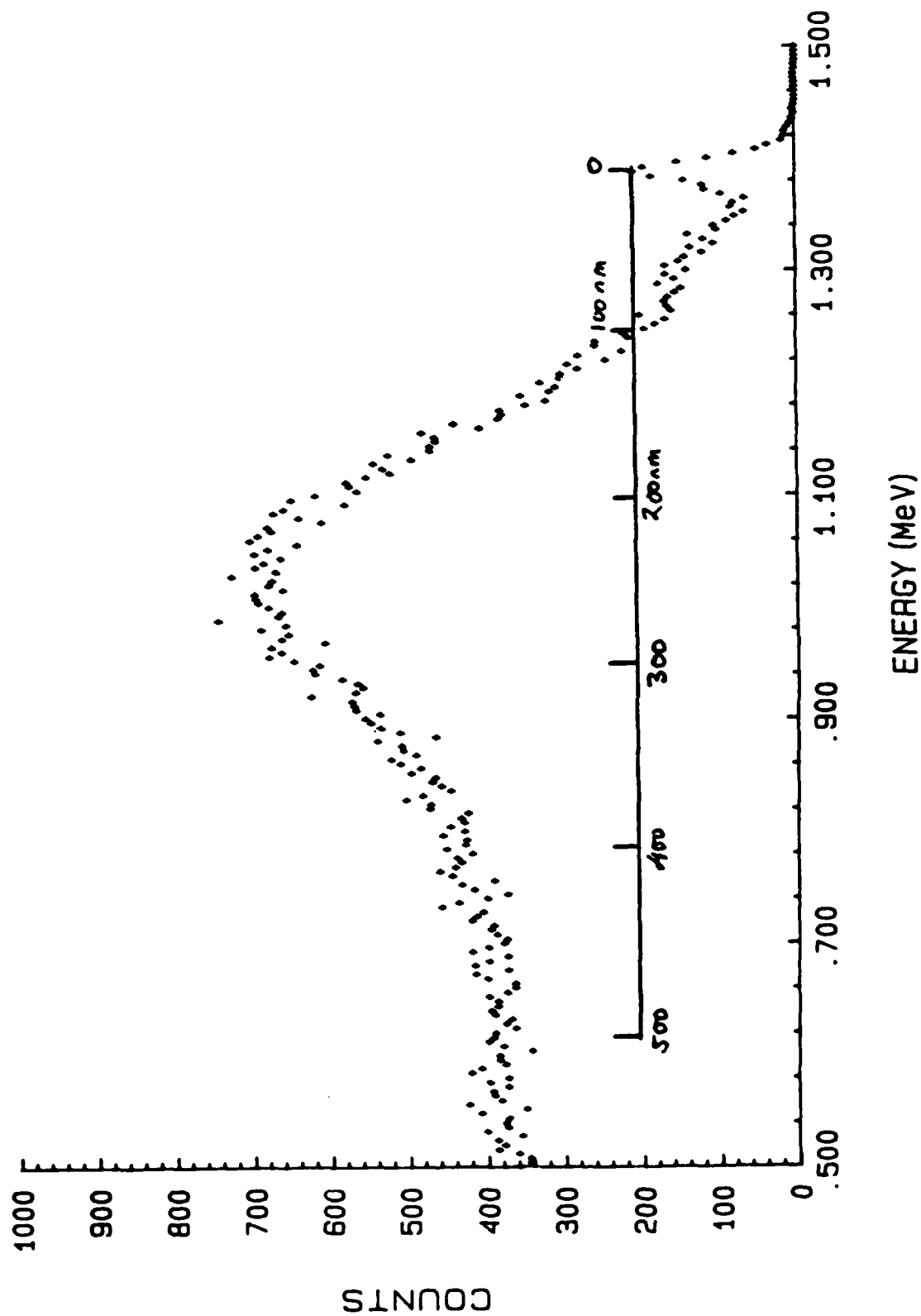


Figure 17. Si Into Si Using Tandetron. 250 keV @ 5×10^{14} . Room Temperature

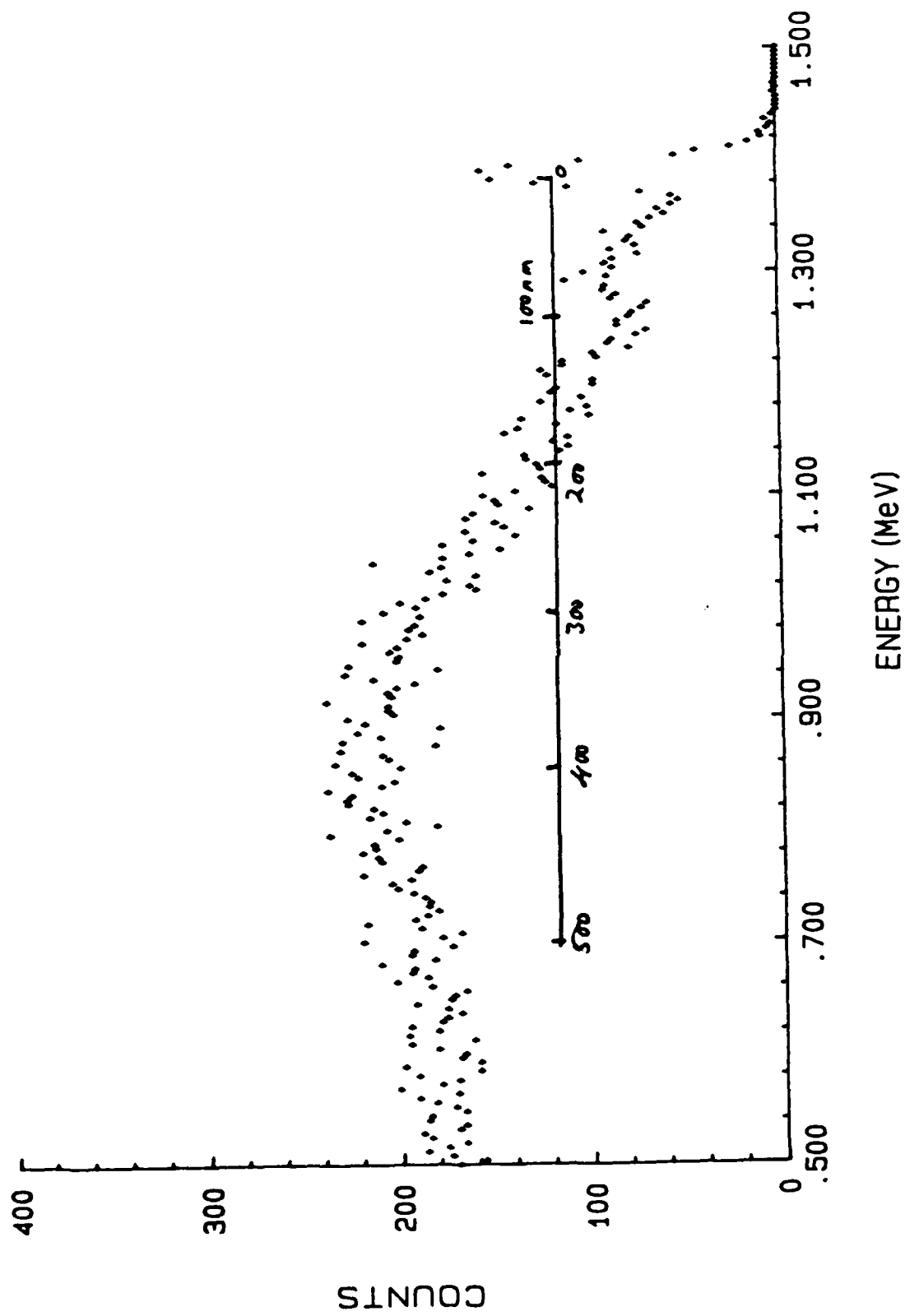


Figure 18. Si Into Si Using Tandetron. 300 keV @ 2×10^{14} Ions/cm². Room Temperature

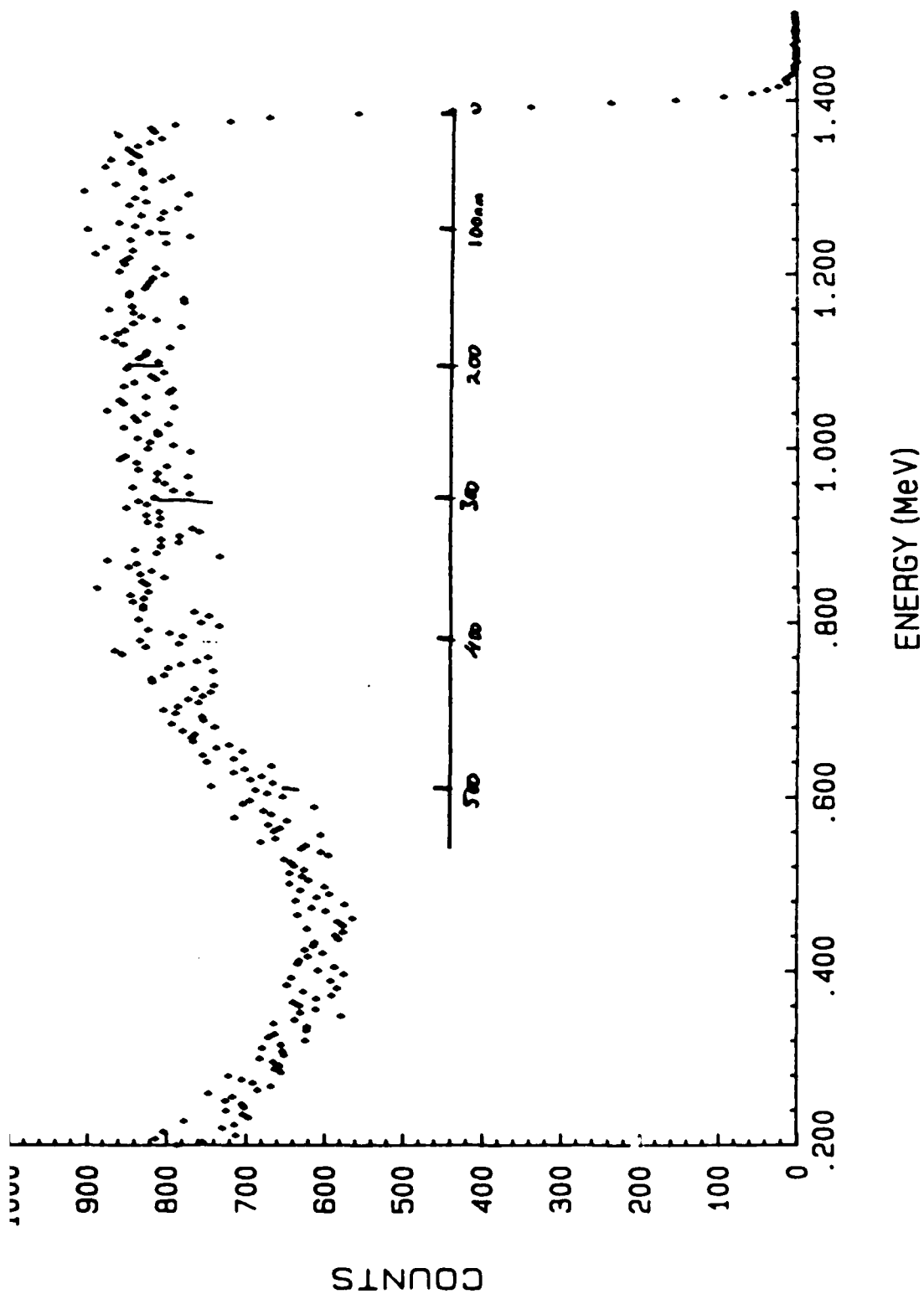


Figure 19. Si Into Si Using Tandetron. 300 keV @ 5×10^{14} Ions/cm². Room Temperature

were mounted with Dow Corning heat sink compound RTV 340, the rest with rubber cement. Both types of mounting were used at 1×10^{15} ions/cm² @ 180 keV. Figure 20 shows the rubber cement mounting. The amorphous region lies between 150 and 250 nm. Figure 21 shows the Dow Corning 340 mounting. In this case the amorphous region extends from about 80 to 300 nm. These two figures show rather dramatically that the rubber cement mounted samples heat up and partially anneal out the amorphous region. Both types of mounting were also used for dosages of 5×10^{14} ions/cm² @ 300 keV. The Dow Corning mount is shown in Figure 22. There is a partially amorphous region between 290 and 390 nm. The rubber cement mounting is shown in Figure 23 with only a slight partially amorphous region. Experimentally the Dow Corning 340 was removed with trichloroethylene. Then the implanted side of the sample was cleaned with four rinses, viz. 1. Basic H, 2. trichloroethylene, 3. acetone, and 4. methanol.

Rubber cemented samples are shown in Figure 24 with 5×10^{14} ions/cm² @ 250 keV and in Figure 25 with 2×10^{14} @ 300 keV. In both cases, apparently enough heat was generated from most of the damage to anneal out. It is interesting to note that at 300 keV, the damage was almost completely annealed out at a dose of 2×10^{14} ions/cm², but not at 5×10^{14} .

A concise summary of the above work is given in Table 2.

To set a upper limit on the temperature rise of an isolated target, we calculate the temperature rise of the target if all the energy of the incident beam is converted into heat. If all the energy of the beam is transferred to heat in the target, then

$$n(\text{ions/cm}^2) E_0(\text{keV}) = C(\text{joules/g K}) \rho (\text{g/cm}^3) t (\text{cm}) \Delta T,$$

where C is the heat capacity, ρ the density, t the thickness, and ΔT is the temperature rise. From Touloukian & Buyco (Reference 39), the heat capacity at room temperature is $C = 0.1650 \text{ cal/g K} = 0.691 \text{ joule/g K}$. The density of silicon is $\rho = 2.3 \text{ g/cm}^3$ and its melting point is $1685 \pm 2 \text{ K}$. $1 \text{ eV} = 1.602 \times 10^{-19} \text{ joules}$.

Thus

$$\Delta T = \frac{n E(\text{in keV})}{t (\text{in cm})} 1.008 \times 10^{-16} \text{ K}$$

REFERENCES (Concluded)

1. H. Ryssel & H. Glawischnig, Ion Implantation Techniques, Springer-Verlag, Berlin, 1982.
2. James F. Gibbons, William S. Johnson & Steven W. Mylroie, Projected Range Statistics - Semiconductors and Related Materials 2nd ed., Dowden, Hutchinson & Ross, Inc., Stroudsburg, PA, 1975.
3. D. K. Brice, Ion Implantation Range and Energy Deposition Distribution. Vol. 1. High Energies, IFI Plenum, NY, 1975.
4. K. B. Winterbon, Ion Implantation Range and Energy Deposition Distributions, Vol. 2 Low Energies, IFI Plenum, NY, 1975.
5. Bernard Smith, Ion Implantation Range Data for Silicon and Germanium Device Technologies, Research Studies Press, Inc., Forest Grove, Oregon, 1977.
6. J. Lindhard, M. Scharff & H. E. Schiott, "Range Concepts and Heavy Ion Ranges," Mat. Fys. Medd. Dan. Vid. Selsk., Vol. 33, p. 14, 1963.
7. G. H. Kinchin & R. S. Pease, "The Displacement of Atoms in Solids by Radiation," Rep. Progr. Phys., Vol. 18, pp. 2-50, 1955.
8. B. L. Crowder & R. S. Title, "The Distribution of Damage Produced by Ion Implantation of Silicon at Room Temperature," Radiation Effects, Vol. 6, pp. 63-75, 1970.
9. See for example, Peter Sigmund, "Collision Theory of Displacement Damage, Ion Ranges, and Sputtering," Rev. Rouman. Physics, Vol. 17(7), 823-870, 1972, and "Collision Theory of Displacement Damage, IV Ion Range and Sputtering," Rev. Rouman. Physics, Vol. 17(8), 969-1000, 1972.
10. F. F. Morehead, Jr. & B. L. Crowder, "A Model for the Formation of Amorphous Si by Ion Bombardment," Radiation Effects Vol. 6, pp. 63-75, 1970.
11. Wei-Kan Chu, James W. Mayer & Marc-A. Nicolet, Backscattering Spectrometry, Academic Press, New York, 1978.
12. Y. S. Touloukian & E. H. Buyco, Thermophysical Properties of Matter, Volume 4: Metallic Elements and Alloys, Plenum, N. Y., 1970.

REFERENCES(Continued)

13. Jun Amano, "Reduction of Crystalline Defects in SOS by Room Temperature Si Ion Implantation," *Radiation Effects*, Vol. 61, pp. 195-200, 1982.
14. Jun Amano & Kent W. Carey, "Low-Defect-Density Silicon on Sapphire," *Journal of Crystal Growth*, Vol. 56, pp. 296-303, 1982.
15. Ronald E. Reedy & Thomas W. Sigmon, "Characterization of Defect Reduction and Aluminum Redistribution in Silicon Implanted SOS Films," *J. Crystal Growth*, Vol. 58, pp. 53-60, 1982.
16. R. E. Reedy, T. W. Sigmon & L. A. Christel, "Suppressing Al Outdiffusion in Implantation Amorphized and Recrystallized Silicon Films," *Appl. Phys. Lett.*, Vol. 42, pp. 707-709, 1983.
17. B. Svensson, J. Linnros & G. Holmen, "Ion Beam Induced Annealing of Radiation Damage in Silicon on Sapphire," *Nucl. Inst. & Methods*, Vols 209/210, pp. 755-760, 1983, also in *Ion Beam Modification of Materials*, 3rd International Conf. on Ion Beam Modification Methods, Grenoble, 6-10 Sept. 1982, B. Biasse, G. Destefanis & J. P. Gailliard, editors, North Holland, Amsterdam, 1983.
18. G. Carter & J. S. Colligon, *Ion Bombardment of Solids*, American Elsevier, NY, 1968.
19. James F. Gibbons, "Ion Implantation in Semiconductors - Part 1: Range Distribution Theory and Experiments," *Proc. IEEE*, Vol. 55, pp. 295-319, 1968 - Part 2: Damage Production and Annealing, *Proc. IEEE* Vol. 60, pp. 1062-1097, 1972.
20. James W. Mayer, Lennart Eriksson & John A. Davies, *Ion Implantation in Semiconductors*, Academic Press, NY, 1970.
21. L. T. Chadderton & F. H. Eisen, editors, *Ion Implantation*, 1st Int. Conf. on Ion Implantation, Gordon & Breach, NY, 1971.
22. Billy L. Crowder, ed., *Ion Implantation in Semiconductors and Other Materials* (3rd Int. Conf. on Ion Implantation in Semiconductors & Other Materials, Yorktown Heights, NY, 1972), Plenum, NY, 1972.
23. Robert G. Wilson & George R. Brewer, *Ion Beams with Applications to Ion Implantation*, Wiley, NY, 1973.
24. G. Dearnaley, J. H. Freeman, R. S. Nelson & J. Stephen, *Ion Implantation*, North Holland, Amsterdam, 1973.
25. Susuma Namba, ed., *Ion Implantation in Semiconductors* (4th Int. Conf. on Ion Implantation in Semiconductors and Other Materials, Osaka, 1974), Plenum, NY, 1974.
26. Fred Chernow, James A. Borders & David K. Brice, *Ion Implantation in Semiconductors 1976* (5th Int. Conf. Boulder, 1976), Plenum, NY, 1976.
27. G. Carter & W. A. Grant, *Ion Implantation of Semiconductors*, Wiley, NY, 1976.

REFERENCES

1. Shinji Onga, Katsunori Hatanaka, Shinji Kawaji & Yukio Yasuda, "Influence of Crystalline Defects and Residual Stress on the Electrical Characteristics of SOS MOS Devices," Jap. J. Appl. Phys. Vol 17, pp. 413-422, 1978.
2. Shinji Onga, Katsunori Hatanaka, Shinji Kawaji, Yoshio Nishi & Yukio Yasuda, "Effect of Residual Stress on Hole Mobility of SOS MOS Devices," Jap. J. Appl. Phys., Vol. 17, pp. 1587-1592, 1978.
3. S. S. Lau, S. Matteson, J. W. Mayer, P. Revesz, J. Gyulai, J. Roth, T. W. Sigmon & T. Cass, "Improvement of Crystalline Quality of Epitaxial Si Layers by Ion-Implantation Techniques," Appl. Phys. Lett, Vol. 34, pp. 76-78, 1979.
4. M. E. Roulet, P. Schwab, I. Golecki & M.-A. Nicolet, "Electrical Properties of Silicon-Implanted Furnace-Annealed Silicon-On-Sapphire Devices," Electronics Letters, Vol. 15, pp. 527-529, 1979.
5. I. Golecki, G. Kinoshita, A. Gat & B. M. Paine, "Recrystallization of Silicon-On-Sapphire by CW Ar Laser Irradiation: Comparison Between the Solid- and the Liquid-Phase Regimes," Appl. Phys. Lett., Vol. 37, pp. 919-921, 1980; Vol. 38, p. 648, 1980.
6. I. Golecki & M.-A. Nicolet, "Improvement of Crystalline Quality of Epitaxial Silicon-On-Sapphire by Ion Implantation and Furnace Regrowth," Solid State Electronics, Vol. 23, pp. 803-806, 1980.
7. I. Golecki, H. L. Glass, G. Kinoshita & T. J. Magee, "Measurements of Defects and Strain in SOS Films After CW Ar Laser Annealing in the Liquid Phase Regime," Applications of Surface Science, Vol. 9, pp. 299-314, 1981.
8. I. Golecki, H. L. Glass & G. Kinoshita, "Reduction in Crystallographic Surface Defects and Strain in 0.2 μm -Thick Silicon-On-Sapphire Films by Repetitive Implantation and Solid-Phase Epitaxy," Appl. Phys. Lett., Vol. 40, pp. 670-672, 1982.
9. Shinji Taguchi, Toshio Yoshii, Yakimasa Ushida & Hiroyuki Tango, "Feasibility Study of SOS VLSI: Capacitance Analysis in Downward Scaling and Improvement of Thin Films by a Solid-Phase Epitaxy," Paper 6-4, 1981 Symposium on VLSI Technology, pp. 92-3.
10. Toshio Yoshii, Shinji Taguchi, Tomoyasu Inoue & Hiroyuki Tango, "Improvement of SOS Device Performance by Solid-Phase Epitaxy," Japanese Journal of Applied Physics, Supplement Vol. 21-1, pp. 175-179, 1982.
11. Tomoyasu Inoue & Toshio Yoshii, "Crystalline Quality Improvement of SOS Films by Si Implantation and Subsequent Annealing," Nuclear Instruments and Methods, Vols. 182/183, pp. 683-690, 1981.
12. Jun Amano & Kent Carey, "A Novel Three-Step Process for Low-Defect-Density Silicon-On-Sapphire," Appl. Phys. Lett., Vol. 39, pp. 163-165, 1981.

SECTION IV

RECOMMENDATIONS

If Dow Corning heat sink compound 340 works at liquid nitrogen temperature, it is a superior mounting medium to rubber cement for amorphization work.

The Tandetron implanter needs a cooling system for targets in order to achieve desired amorphous regions. This project is already under way and should be in use before this report is printed.

SECTION III SUMMARY AND CONCLUSIONS

A number of Si into Si implant conditions were studied to ascertain the conditions necessary to amorphize 0.3 and 0.5 micron thick Si films for subsequent recrystallization studies. The conditions found for the Avionics Laboratory, Varian 400-10AR Ion Implanter are all cases where the sample was mounted with rubber cement and the dewar was filled with liquid nitrogen. Later studies suggest that Dow Corning heat sink compound RTV 340 is a superior mounting arrangement, especially at room temperature. For 0.3 micron thick Si films, the best combinations for amorphizing the film are:

5×10^{14} ions/cm ²	@ 150 keV
5×10^{14}	@ 180
2×10^{14}	@ 200.

For 0.5 micron thick Si films, the combinations are:

5×10^{14} ions/cm ²	@ 250 keV
5×10^{14}	@ 275 (maybe no surface left for seed)
$2 \times 10^{14} / 2 \times 10^{14}$	@ 300 keV/120 keV.

Apparently most samples run on the Tandetron, which had no means of cooling samples, heated up and annealed out much of the amorphous region except for the lowest energy and dosage case of 5×10^{14} ions/cm² @ 180 keV which gave results similar to the Varian. Substrate temperature appears to be as important a parameter as ion energy and dosage in determining the depth and amount of amorphization.

If we assume that the thermal conductivity is high enough for complete heat dispersion, we have $t = 0.05$ cm, $n = 5 \times 10^{14}$ ions/cm², and $E = 200$ keV, $\Delta T = 202$ K.

The typical SOI case has a silicon film on an insulating substrate, thus if we had a 0.5 micron thick films, $\Delta T = 2.02 \times 10^5$ K, more than enough to melt the film. The RBS results on uncooled samples indicate an anneal which must have reached 500 to 1000°C. Thus we conclude that much of the heat generated must have been localized in the region of damage.

TABLE 2 (Concluded)

Energy in keV	Dose $\div 10^{14}$ ions/cm ²	Depth of region amorphized
1.7 Mev Tandetron accelerator (all samples room temperature and above)		
180	10	60-280 nm
250	5	200-260 nm ? maybe only partially
300	2	pretty much like single crystal
300	5	pretty much like single crystal

TABLE 2. SUMMARY OF Si⁺ IMPLANT CONDITIONS STUDIED. ALSO REGION OF DEPTH WHERE TARGET IS AMORPHIZED

Energy in keV	Dose $\times 10^{14}$ ions/cm ²	Sample Temperature	Depth of region amorphized
VARIAN 400-10AR Ion Implanter (all samples mounted with rubber cement except last two where Dow Corning heat sink compound RTV 340 was used)			
150	1	LN ₂	region around 130nm partially amorphized
150	2	LN ₂	100-160 nm ?
150	5	LN ₂	0-220 nm
180	5	LN ₂	0-280 nm
180	10	LN ₂	0-325 nm
200	0.5	LN ₂	-
200	1	LN ₂	region around 220 nm partially amorphized
200	2	LN ₂	80-230 nm
200	5	LN ₂	50-320 nm
250	1	LN ₂	region around 220 nm partially amorphized
250	2	LN ₂	120-300 nm
250	5	LN ₂	0-375 nm
275	5	LN ₂	0-380 nm
275	10	LN ₂	0-400 nm
300	2	LN ₂	100-450 nm
300/120	2/2	LN ₂	0-450 nm
300	5	LN ₂	0-420 nm ?
325	10	LN ₂	20-500 nm
180	10	RT	150-250 nm
250	5	RT	pretty much like single crystal
300	2	RT	pretty much like single crystal
300	5	RT	region around 400 nm partially amorphized
180	10	RT	90-300 nm
300	5	RT	region around 330 nm partially amorphized

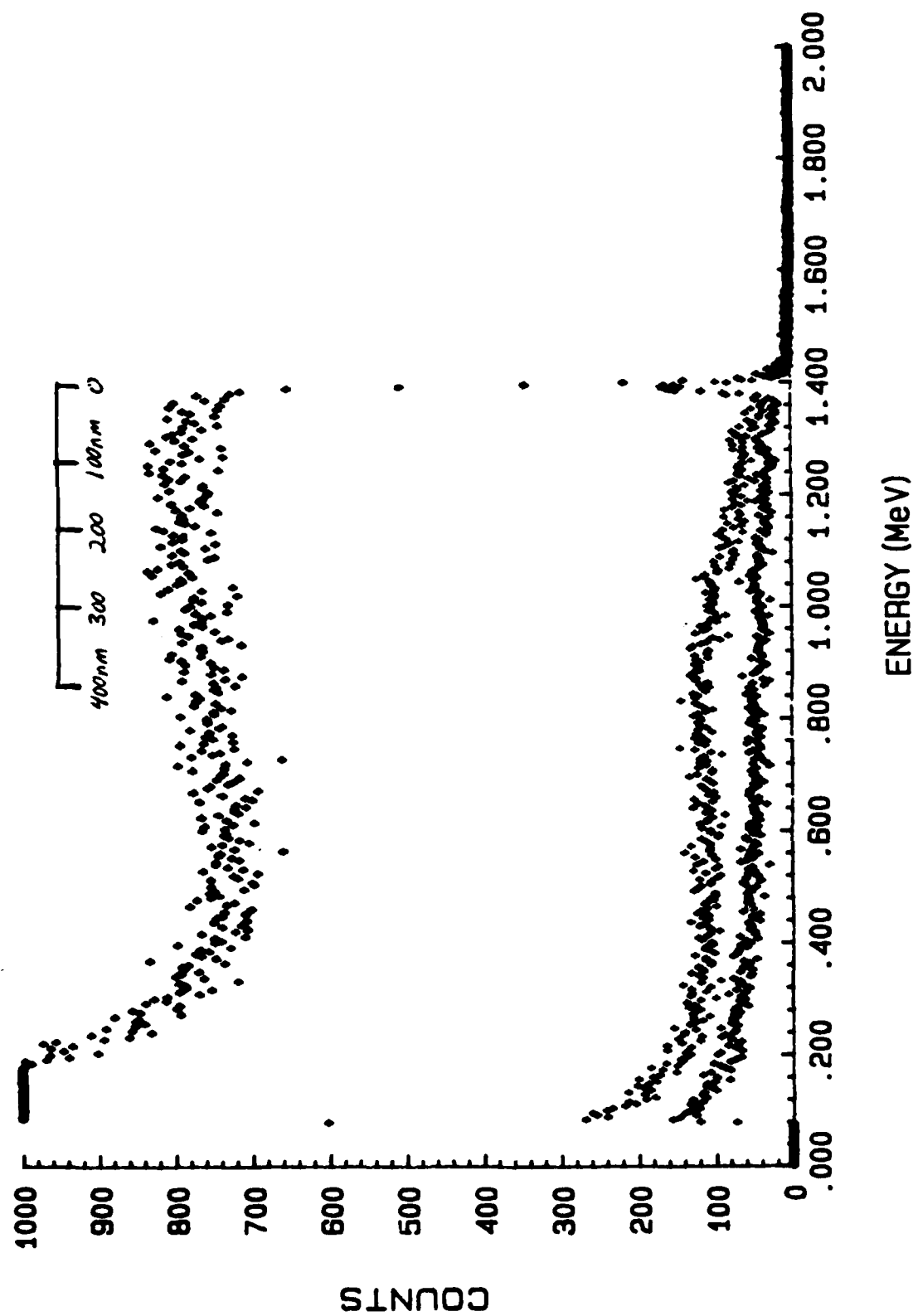


Figure 25. Si In to Si On Varian Machine. 300 keV @ 2×10^{14} Ions/cm². Rubber Cement Mounting. Room Temperature

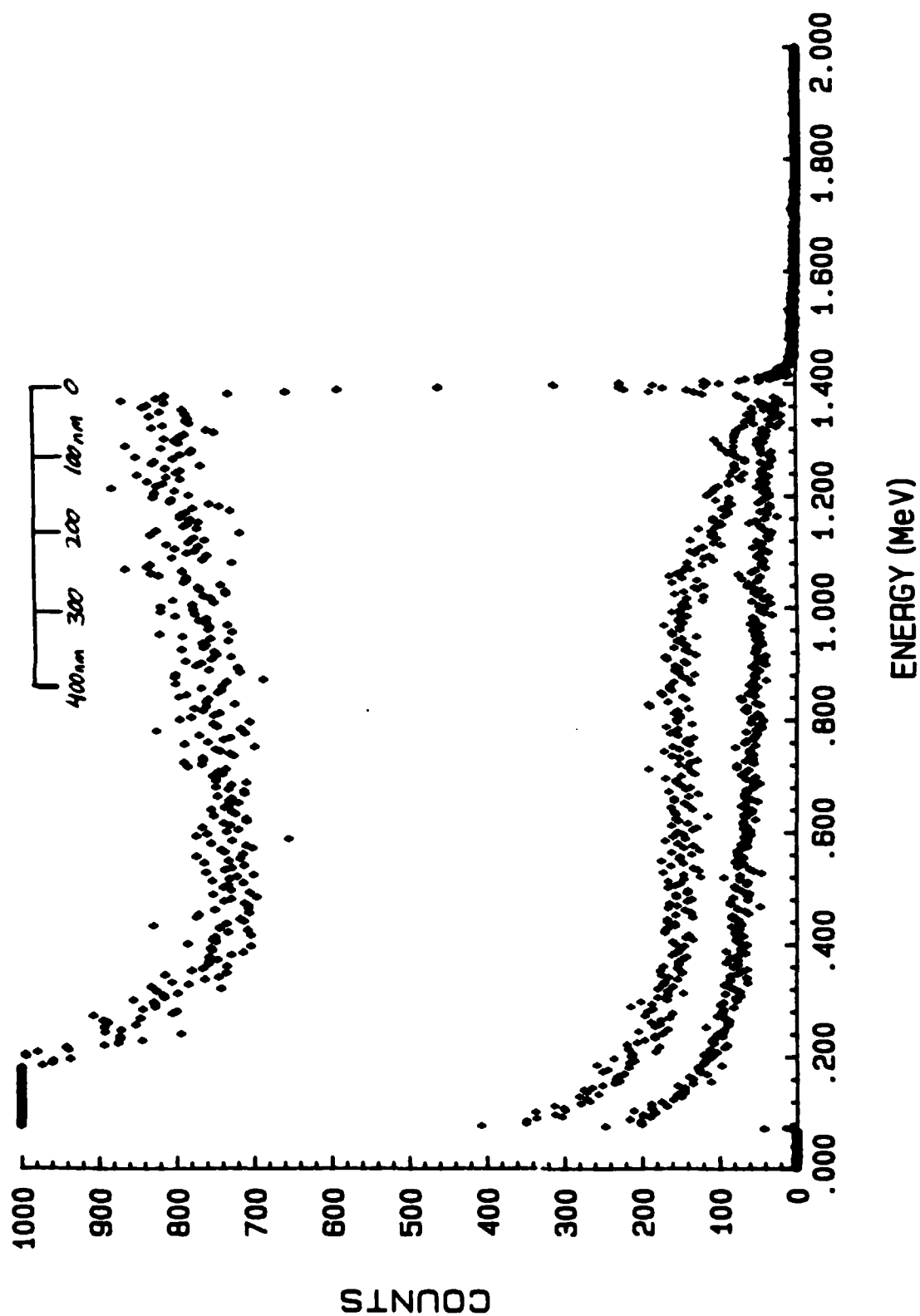


Figure 24. Si Into Si On Varian Machine. 250 keV @ 5×10^{14} Ions/cm². Rubber Cement Mounting. Room Temperature

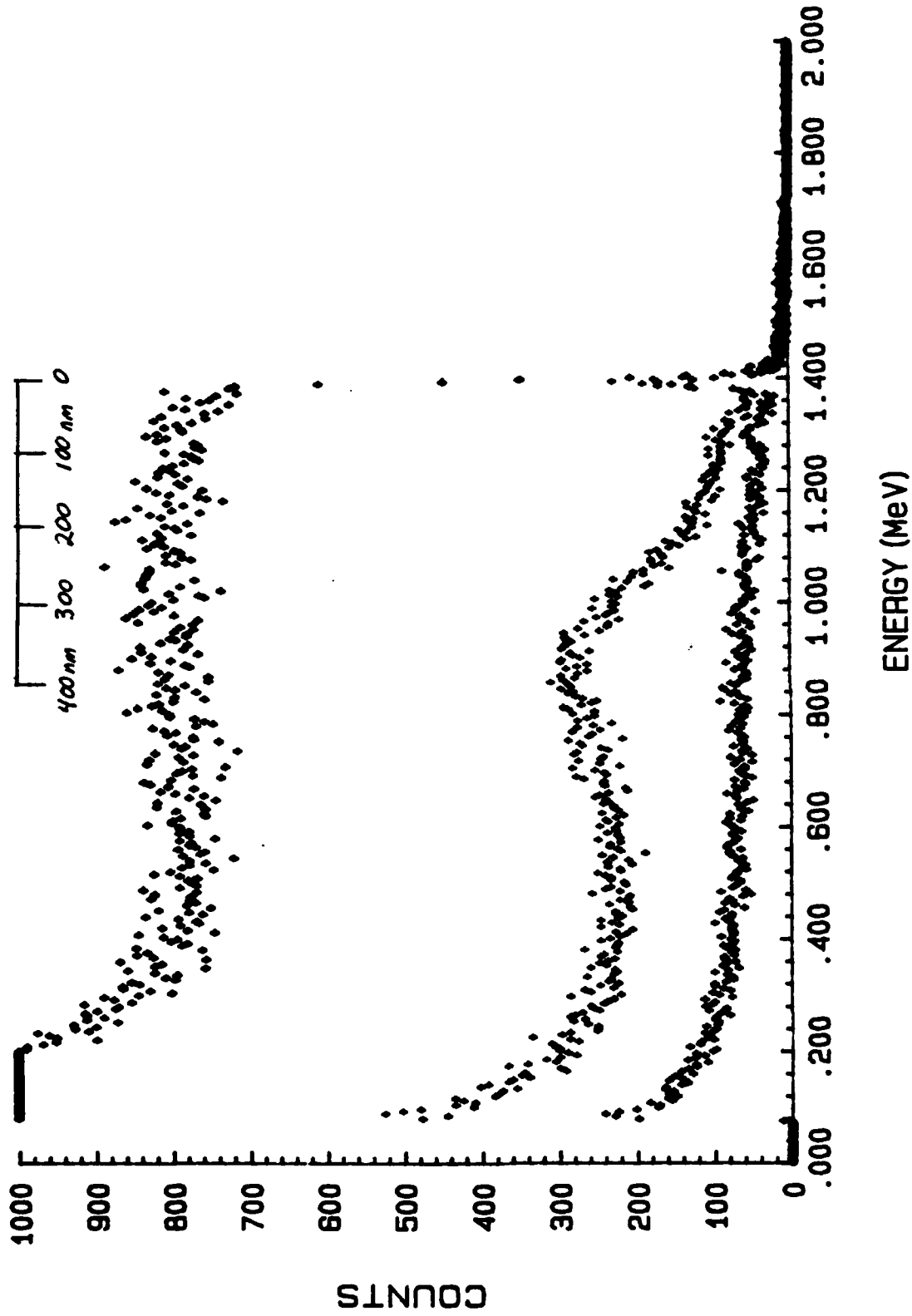


Figure 23. Si Into Si On Varian Machine. 300 keV @ 5×10^{14} Ions/cm². Rubber Cement Mounting. Room Temperature

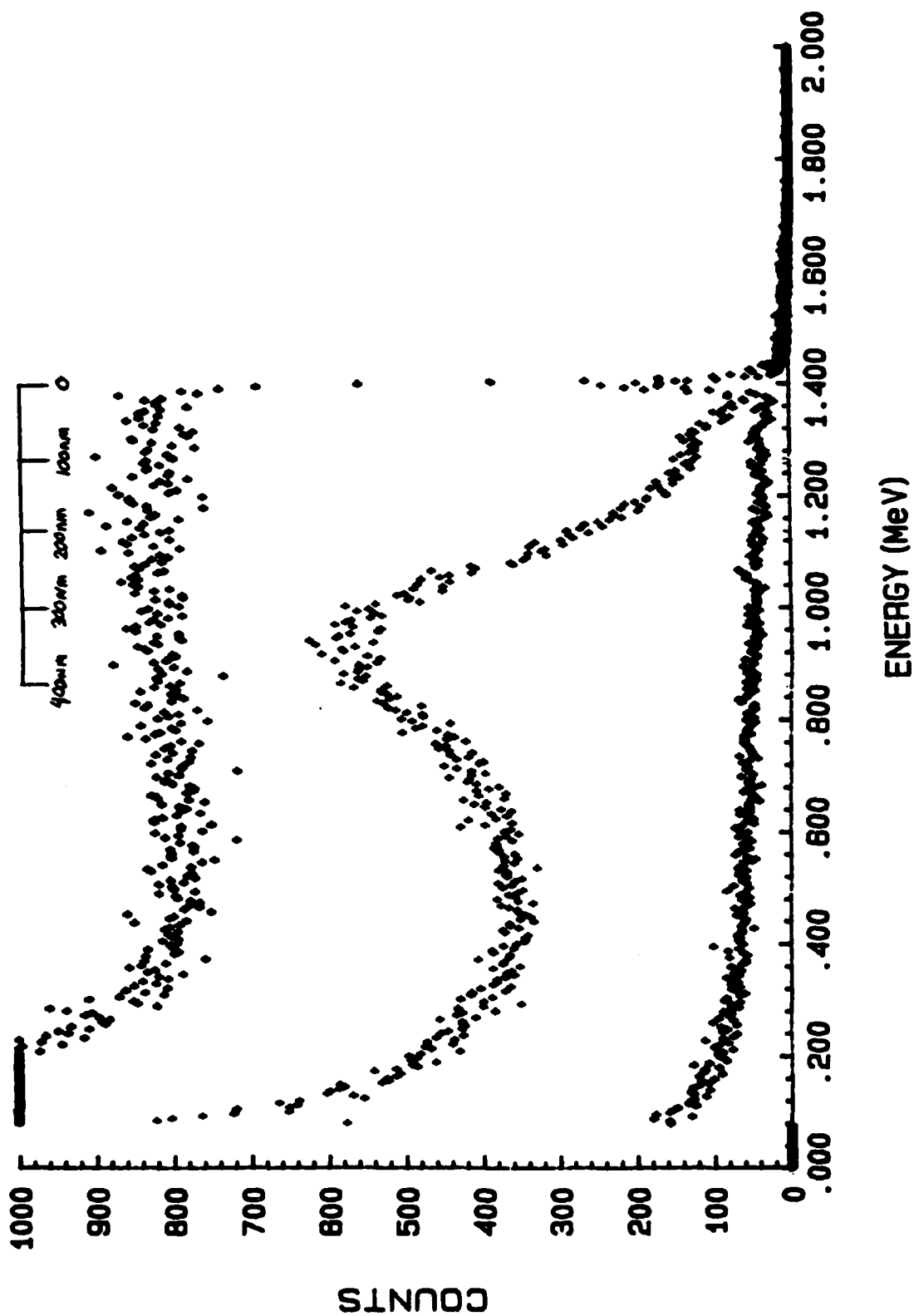


Figure 22. Si Into Si On Varian Machine. 300 keV @ 5×10^{14} Ions/cm². Dow Corning 340 Mounting. Room Temperature

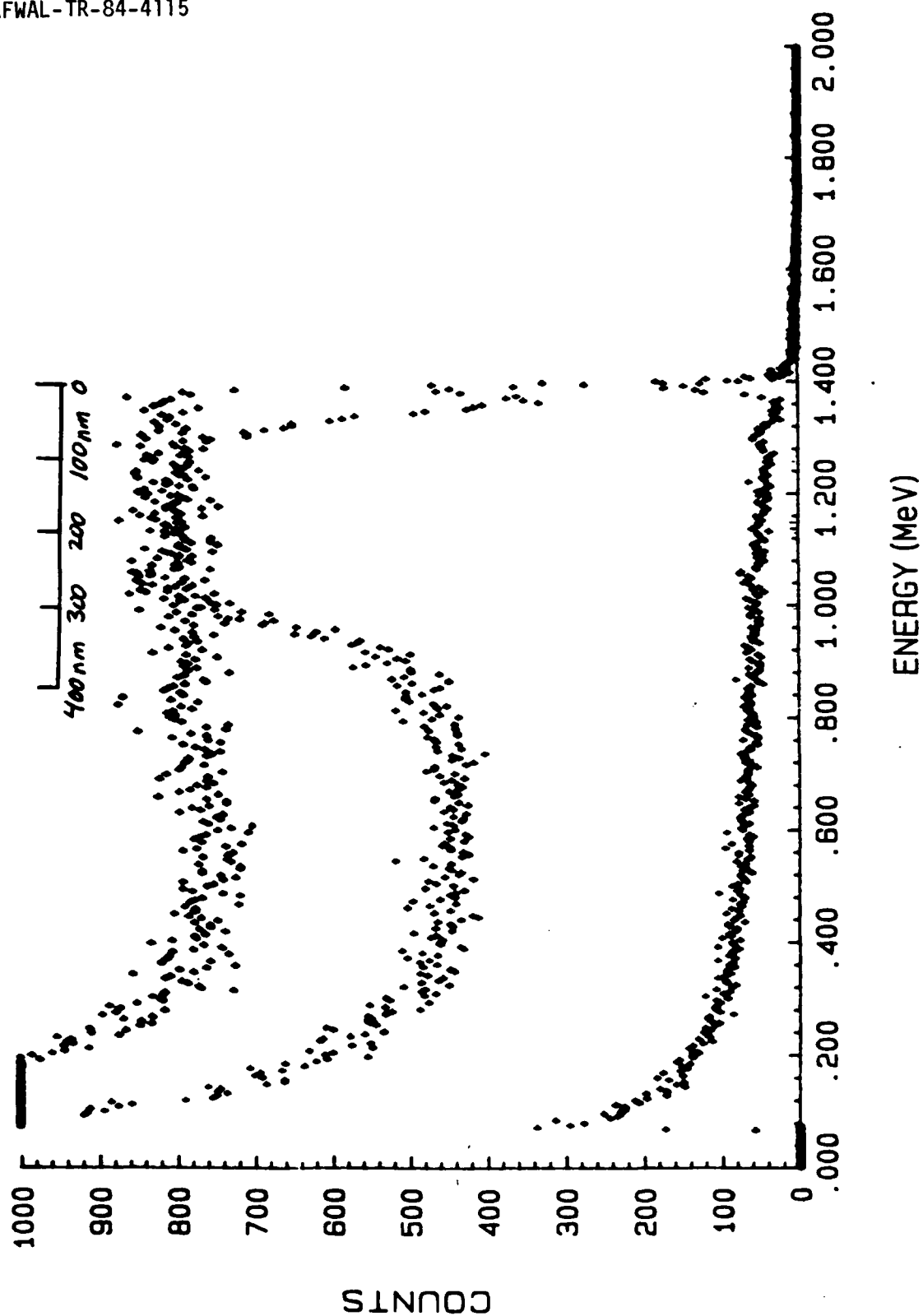


Figure 21. Si Into Si Implants Using Varian Machine. 180 keV Incident Ion Beam
Energy With 1×10^{15} Ions/cm² Dose. Rubber Cement Mounting. Initially
at Room Temperature

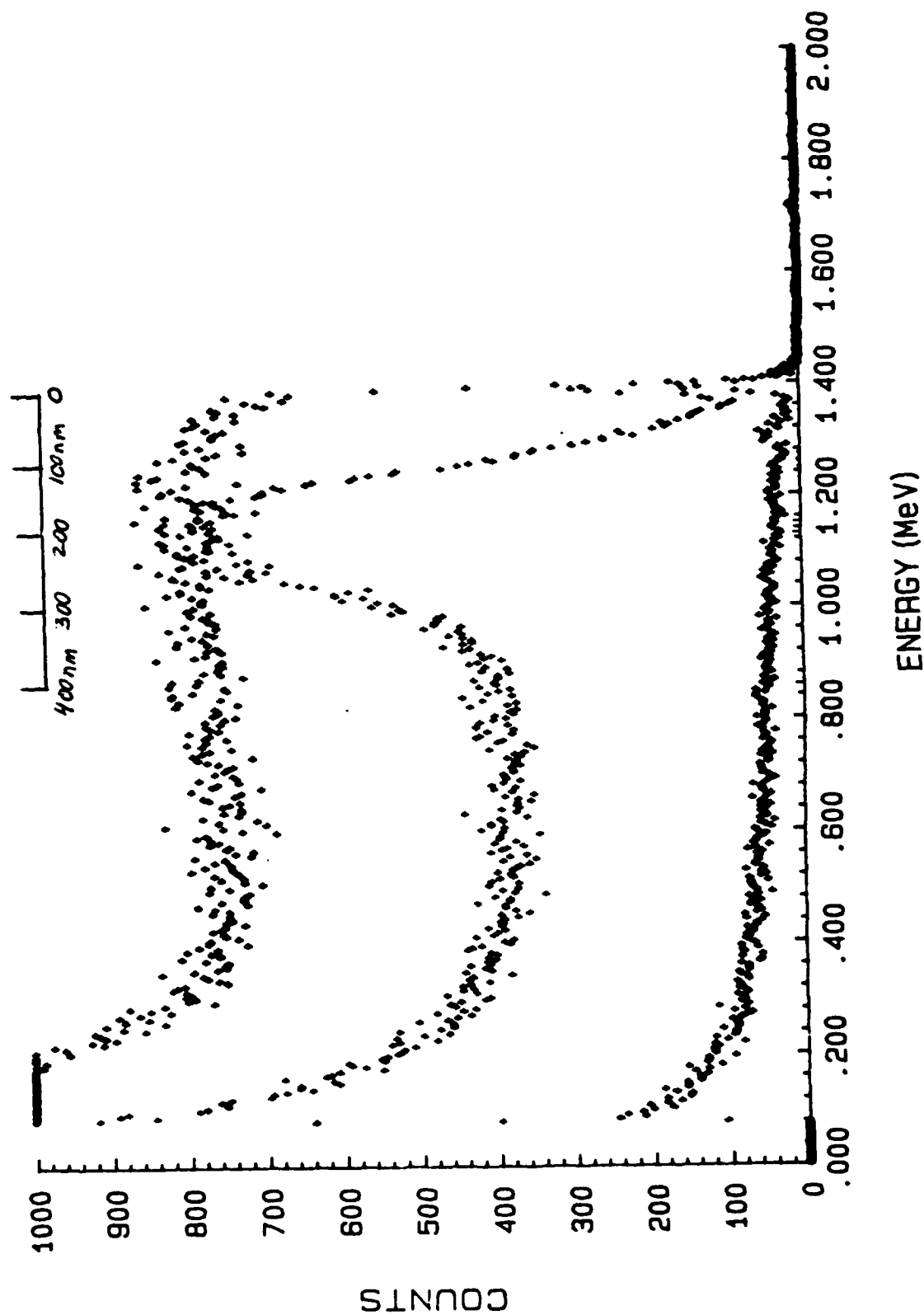


Figure 20. Si Into Si Using Varian Machine. 180 keV Incident Ion Beam Energy With
 1×10^{15} Ions/cm² Dose. Dow Corning 340 Mounting. Room Temperature

END

FILMED

10-85

DTIC